# Numerical Investigation of the Lateral Response of Horizontally Loaded Single Pile Embedded in Layered Soil

Berhanu Weyo Ogato

A Thesis Submitted to Civil Engineering Department
School of Civil Engineering and Architecture

Presented in Partial Fulfillment of the Requirement for the award of Degree of Master's in Civil Engineering (Specialization in Geotechnical Engineering)

Office of Graduate Studies
Adama Science and Technology University

June, 2023
Adama, Ethiopia

# Numerical Investigation of the Lateral Response of Horizontally Loaded Single Pile Embedded in Layered Soil

Berhanu Weyo Ogato

Advisor: Argaw Asha (PhD)

A Thesis Submitted to

Civil Engineering Department
School of Civil Engineering and Architecture

Presented in Partial Fulfillment of the Requirement for the award of Degree of Master's in Civil Engineering (Specialization in Geotechnical Engineering)

Office of Graduate Studies
Adama Science and Technology University

June, 2023
Adama, Ethiopia

# Declaration

I hereby declare that this Master Thesis entitled "Numerical Investigation of the Lateral Response of Horizontally Loaded Single Pile Embedded in Layered Soil" is my original work. That is, it has not been submitted for the award of any academic degree, diploma, or certificate in any other university. All sources of materials that are used for this thesis have been duly acknowledged through citation.

| | | |
|---|---|---|
| Berhanu Weyo Ogato | ______________________ | ____________________ |
| Name of Student | Signature | Date |

# Recommendation

I, the advisor of this thesis, hereby certify that I have read the revised version of the thesis entitled "Numerical Investigation of the Lateral Response of Horizontally Loaded Single Pile Embedded in Layered Soil" prepared under my guidance by Berhanu Weyo submitted in partial fulfillment of the requirements for the degree of Masters of Science in Civil Engineering (Geotechnical Engineering). Therefore, I recommend the submission of revised version of the thesis to the department following the applicable procedures.

| | | |
|---|---|---|
| Argaw Asha (PhD) | ______________________ | 13/06/2023 |
| Major-Advisor | Signature | Date |

# Approval Page of M.Sc. Thesis

I, the advisors of the thesis entitled "Numerical Investigation of the Lateral Response of Horizontally Loaded Single Pile Embedded in Layered Soil" developed by Berhanu Weyo, hereby certify that the recommendation and suggestions made by the board of examiners are appropriately incorporated into the final version of the thesis.

| | | |
|---|---|---|
| Argaw Asha (PhD) | ____________________ | 13/06/2023 |
| Major-Advisor | Signature | Date |

We, the undersigned, members of the Board of Examiners of the thesis by Berhanu Weyo have read have read and evaluated the thesis entitled "Numerical Investigation of the Lateral Response of Horizontally Loaded Single Pile Embedded in Layered Soil" and examined the candidate during open defense. This is, therefore, to certify that the thesis is accepted for partial fulfillment of the requirement of the degree of Master of Science in Civil Engineering (Specialization in Geotechnical Engineering).

| | | |
|---|---|---|
| ____________________ | ____________________ | ____________________ |
| Chairperson | Signature | Date |
| ____________________ | ____________________ | ____________________ |
| Internal Examiner | Signature | Date |
| ____________________ | ____________________ | ____________________ |
| External Examiner | Signature | Date |

Final approval and acceptance of the thesis is contingent upon submission of its final copy to the Office of Postgraduate Studies (OPGS) through the Department Graduate Council (DGC) and School Graduate Committee (SGC).

| | | |
|---|---|---|
| ____________________ | ____________________ | ____________________ |
| Department head | Signature | Date |
| ____________________ | ____________________ | ____________________ |
| School Dean | Signature | Date |
| ____________________ | ____________________ | ____________________ |
| Office of Postgraduate Studies, Dean | Signature | Date |

# ACKNOWLEDGEMENT

I would like to forward my deepest gratitude to my advisor Dr. Argaw Asha for his critical observations, suggestions, comments, and endless support at various stage of this thesis work.

I also express my sincere thanks to Adama Science and Technology Geotechnical Engineering staff for their comments, encouragements, and many useful contributions in my study. I really appreciate their support for every helpful assistance they have made for me during the period of my study.

I would like to forward my heartfelt thanks to ARCOON DESIGN BUILD P.L.C, who gave me soil data for my thesis.

I thank all staffs of the Civil Engineering Department for their encouragements during my thesis work.

# Table of Contents


Table of Contents ..... i
List of Tables ..... iv
List of Figures ..... v
List of Acronyms and Abbreviations ..... vii
Abstract ..... viii
1. INTRODUCTION ..... 1
1.1. General Background ..... 1
1.2. Statement of the Problem ..... 2
1.3. Objective ..... 2
1.3.1. General Objective ..... 2
1.3.2.Specific Objectives ..... 2
1.4. Scope of the Study ..... 3
1.5. Significance of the study ..... 3
1.6. Organization of Thesis ..... 3
2.LITERATURE REVIEW ..... 5
2.1. Introduction ..... 5
2.2. Load Transfer Mechanisms (Statics) of Piles ..... 6
2.3. Kinematics and Failure Modes of Laterally Loaded Piles ..... 8
2.4. Analysis Methods ..... 10
2.4.1. Broms Method (1964a and 1964b) ..... 11
2.4.2. Subgrade Reaction Approach ..... 18
2.4.3. Continuum Method ..... 25
2.5. Ultimate Lateral Resistance ..... 31
2.6. Constitutive Models ..... 32
2.6.1. Linear Elastic Model ..... 33
2.6.2.Mohr Coulomb Model ..... 33
3. Materials and Methods ..... 36
3.1. General description of study area ..... 36
3.1.1. Location ..... 36

3.1.2. Geology and Subsurface Condition ..... 36
3.2. Methodologies ..... 38
3.3. Parameters used for the base model ..... 38
3.3.1. Soil parameters ..... 38
3.4. Parameters of reinforced concrete circular pile used for the model ..... 39
4. Numerical Modeling ..... 42
4.1. Introduction ..... 42
4.2. Overview of PLAXIS 3D FOUNDATION ..... 42
4.3. Generation of the Model ..... 45
4.3.1. Model Geometry ..... 45
4.3.2. Model Properties ..... 46
4.3.3. Model Boundary Fixities ..... 47
4.3.4. Mesh Generation ..... 48
4.3.5. Sensitivity Analysis ..... 51
4.3.6. Calculation Process ..... 51
4.3.7. Interface Element ..... 53
4.4. Validation of Numerical Model ..... 55
5. ANALYSIS AND PARAMETRIC STUDIES ..... 57
5.1. Introduction ..... 57
5.2. Results and Discussion ..... 57
5.2.1. Effect of Pile Diameter on Head Deflection ..... 57
5.2.2. Effect of Length of the Pile on Head Deflection ..... 59
5.2.3. Effects of Loading Eccentricity, e on Head Deflection ..... 60
5.3. Ultimate Lateral Load Capacity from Numerical Results ..... 62
5.3.1. Effect of Diameter of the Pile on Lateral Load Capacity ..... 63
5.3.2.Effect of Length of the Pile on Lateral Load Capacity ..... 65
6. CONCLUSIONS AND RECOMMENDATIONS ..... 68
6.1. Conclusions ..... 68
6.2. Recommendations ..... 70
References ..... 71
Appendix A - Geotechnical properties of soil ..... 75

Appendix B - Ultimate Capacity from Numerical Results .......... 81
Appendix C- Plaxis out .......... 82

# List of Tables

Table 3.1: Soil Parameters for Base Model from SPT correlation. .............................................. 39
Table 3.2: Pile parameters.......................................................................................................... 40
Table 3.3: Pile diameters and lengths ......................................................................................... 41
Table 4.1: 3D FEM model dimensions (design of experiments) ................................................ 46
Table 4.2: Influence of mesh size on head deflection ................................................................ 51
Table 4.3: Geotechnical properties of the soil layer ................................................................... 55
Table A. 1: Typical values SPT - Based soil and rock classification systems (Skempton, 1986) 75
Table A .2: Typical values of Young's modulus (MPa) for granular materials (Kézdi&Réthái, 1974 and Prat et al., 1995) ........................................................................................................ 75
Table A.3: Typical values of Young's modulus (MPa) for cohesive materials (Kézdi and Réthái, 1974 and Prat et al., 1995) ........................................................................................................ 76
Table A.4: Typical values of Poisson’s ratio for soils and other material, Bowels (1977) .......... 76
Table B.1: Lateral load capacity and lateral deflection .............................................................. 81
Table C.1: Pile length of 15m ...................................................................................................... 82
Table C.2: Pile length of 20m ...................................................................................................... 83
Table C.3: Pile length of 25m ...................................................................................................... 84
Table C.4: Pile length of 30m ...................................................................................................... 85

# List of Figures


Figure 2.1: Load Transfer Mechanism of Axially Loaded Piles after (Basu et al., 2008)............. 7
Figure 2.2: Load Transfer Mechanism of Laterally Loaded Piles (Basu et al., 2008).................... 8
Figure 2.3: Kinematics of Rigid Piles........................................................................... 9
Figure 2.4: Kinematics of Flexible Piles........................................................................ 9
Figure 2.5: Broms Earth Pressures for Cohesive Soils ............................................................ 12
Figure 2.6: Broms Pressure, Shear, Moment Diagrams for Cohesive Soils ............................... 12
Figure 2.7: Broms Pressure, Shear, Moment Diagrams for Cohesionless Soils........................... 15
Figure 2.8: Ultimate lateral resistance of short pile in cohesive soil .......................................... 16
Figure 2.9: Ultimate lateral resistance of long pile in cohesive soil ........................................... 17
Figure 2.10: Charts for calculation of lateral deflection at ground surface of horizontally loaded pile in cohesive soil (after Broms 1964). ....................................................................... 18
Figure 2.11: A Beam on an Elastic Foundation (after Ermi Winkler)........................................ 19
Figure 2.12: Critical length for a laterally loaded pile after (Lymon C.Reese and William F.Van Impe, 2011). ......................................................................................................... 22
Figure 2.13: Schematic diagram of (H.G.Poulos and E.H.Davis, 1980) method ........................ 27
Figure 2.14: Load test result (Briaud, 2013)....................................................................... 32
Figure 2.15: Basic idea of an elastic perfectly plastic model (R.B.J. Brinkgreve and W. Broere, 2006) ................................................................................................................ 34
Figure 2.16: The Mohr-Coulomb yield surface in principal stress space (c = 0) (R.B.J. Brinkgreve and W. Broere, 2006)................................................................................................. 35
Figure 4.1: General three-dimensional coordinate system and sign convention for the model.... 43
Figure 4.2:3D finite element mesh for soil mass and location of pile. ........................................ 45
Figure 4.3: Boundary conditions.................................................................................... 48
Figure 4.4: Local numbering and positioning of nodes (•) and integration points (x) of a 10-node wedge element in Plaxis 3D Foundation (Plaxis 3D Foundation Manual, 2006)........................ 49
Figure 4.5: Mesh generation of the cross section of a typical 2D FE model ............................... 50
Figure 4.6: Mesh generation of a typical 3D FE model............................................................. 50
Figure 4.7: Calculation phases in Plaxis 3D Foundation ........................................................... 53
Figure 4.8: Local numbering and positioning of nodes (Ɛ) and integration points (x) of a 16-node interface element (Plaxis 3D Foundation Manual, 2006) .......................................................... 54

Figure 4.9: Comparison of finite element result with field test data from (F.Ismael, 1998). ....... 56
Figure 5.1: Lateral load versus head deflection of 15m pile length............................................. 58
Figure 5.2: Lateral load versus head deflection of 20m pile length............................................. 58
Figure 5.3: Lateral load versus head deflection of 25m pile length............................................. 59
Figure 5.4: Lateral load versus head deflection of 30m pile length............................................. 59
Figure 5.5: Lateral load versus head deflection of 15m pile length............................................. 60
Figure 5.6: Lateral load versus head deflection of 20m pile length............................................. 61
Figure 5.7: Lateral load versus head deflection of 25m pile length............................................. 61
Figure 5.8: Lateral load versus head deflection of 30m pile length............................................. 62
Figure 5.9: The effect of change in diameter on lateral capacity pile with length 15m. .............. 63
Figure 5.10: The effect of change in diameter on lateral capacity pile with length 20m. ............ 64
Figure 5.11: The effect of change in diameter on lateral capacity pile with length 25m. ............ 64
Figure 5.12: The effect of change in diameter on lateral capacity pile with length 30m. ............ 65
Figure 5.13: The effect of change in length on lateral capacity pile with diameter 0.5m. ........... 66
Figure 5.14: The effect of change in length on lateral capacity pile with diameter 0.8m. ........... 66
Figure 5.15: The effect of change in length on lateral capacity pile with diameter 1.1m. ........... 67
Figure 5.16: The effect of change in length on lateral capacity pile with diameter 1.4m. ........... 67
Figure A.1:Borehole log sheet ..................................................................................... 79
Figure A.2: Cross section............................................................................................. 80

# List of Acronyms and Abbreviations

| | |
|---|---|
| FEM | Finite Element Method |
| 3D | Three Dimensional |
| 2D | Two Dimensional |
| SPT | Standard Penetration Test |
| USCS | Unified Soil Classification System |

# Abstract

*The piles are subjected to lateral loads which may generated by wind, earthquake, water current, earth pressure, effect of moving vehicles or ships, plant, and equipment. The accurate prediction of lateral response of pile is important design criteria due to changes in load carrying mechanism. The objective of this thesis is to analyze the performance of laterally loaded pile through a parametric study embedded in layered soil of Addis Ababa city around Bole area. Full-scale field test result obtained from the literature was used for the validation of Plaxis 3D Foundation FEM. A parametric study was conducted by varying pile diameter, length and loading eccentricity. PLAXIS 3D FOUNDATION V.1.1 was used as a tool to carry out all the analysis of parameters.*

*The result shows that the changes in the pile diameter and loading eccentricity have the great effect on the horizontal displacement of the pile and ultimate resistance of the pile. The head deflection of the pile decreased by 66.02% when the pile diameter increases from 500mm to 800mm and increasing the load eccentricity from 0 to 1m increases the pile head deflection by 34% for the highest load. The findings contribute to understanding pile behavior and provide valuable insights for the analysis of single piles in practical engineering applications. Further studies are needed to establish other parameters and see their effect.*

***Key words: Laterally Loaded Piles; Layered Soil; Plaxis 3D Foundation***

# 1. INTRODUCTION

## 1.1. General Background

Piles are becoming increasingly popular due to economic development, providing high load bearing capacity, small uneven settlement, and anti-liquefaction.

Piles are subjected to lateral loads which can be generated by wind, earthquake, water current, earth pressure, moving vehicles or ships, plant, and equipment. The load carrying mechanism changes when the pile is subjected to lateral loads, which is resisted by the soil–pile interaction effect (Rollins and Sparks, 2002). In these cases, the primary function of piles is to transfer lateral loads to the ground. An appropriate understanding of the response of pile under lateral loading has a great importance and complex problem, as the mechanism of transfer of lateral loads to the subsurface strata is dependent on the characteristics of sub-soil and pile itself. Hence, a proper concept of load transfer mechanism of pile to soil is required for analysis and design.

The lateral load capacity of pile foundations is essential for the design of civil structures. There have been many studies on the behavior of piles subjected to lateral loading. Experimental studies have been carried out to investigate the behavior of piles under various loading conditions. However, these studies are costly and time-consuming. Numerical modeling provides a cost-effective alternative to experimental studies. Finite element modeling has been widely used to investigate the behavior of pile foundations under various loading conditions. A lot of methods have been developed to predict the lateral capacity of single piles under static loads, but there is little information to guide engineers in the design of eccentrically loaded piles embedded in layered soil.

This study investigates the behavior of laterally loaded pile foundation for soil sites found in Addis Ababa city. A parametric study was conducted to see the effect of pile diameter, pile length, and loading eccentricity on response of laterally loaded pile foundation. Finite Element Method modelling was used to account for the complex geometry and interaction of pile foundation. Therefore, this thesis focuses on examining the effects of these variables.

## 1.2. Statement of the Problem

The response of laterally loaded pile foundation is very important in the design of civil engineering structures. Piles are used to support lateral soil movement under an embankment, unstable soil layers or nearby vertical excavation activities, bridge abutments, moving slopes and structures subjected wind loads. Piles may be designed to support laterally loaded structures. There is a limited literature about the lateral response of eccentrically loaded pile and this is the gap that impose this research.

Therefore, it is very important to investigate the response of laterally loaded single pile embedded in layered soil. To address the response of the pile, parametric study was conducted using loading eccentricity, pile diameter, and length embedded in soil data taken from Addis Ababa where high-rise buildings were constructed.

## 1.3. Objective

### 1.3.1. General Objective

The main objective of this thesis is investigation of the lateral response of horizontally loaded Single pile embedded in layered soil by using PLAXIS 3D FOUNDATION V.1.1 finite element software.

### 1.3.2. Specific Objectives

The specific objectives of this thesis are:

- To evaluate the influence of pile length and diameter on the static laterally loaded response of single pile.
- To investigate the effect of loading eccentricity on the lateral response of the pile
- Providing nearly accurate predictions of the ultimate lateral loading capacity of pile by using pile diameter, length and loading eccentricity as parametric study which are important design criteria in the analysis and design of pile foundations.

## 1.4. Scope of the Study

This study investigates the lateral response of single pile loaded horizontally by using three-dimensional finite element software PLAXIS 3D FOUNDATION V1.1. The soil profile used for the analysis is taken from Addis Ababa where high-rise buildings have been already constructed. This study is limited to investigate the effects of loading eccentricity, pile diameter, and length on pile lateral displacement and ultimate lateral resistance when pile is subjected to static horizontal loads.

Elastic-perfectly plastic Mohr-Coulomb failure criterion was used in all analyses of soil and rock. The supporting purpose is assumed for long period and soil is in drained condition for all layers. The effect of water, the stress changes, the effect of heave and vertical settlements are not in the scope of this thesis.

## 1.5. Significance of the study

Present studies (S. Karthigeyan et al., 2007) and (Wong et al., 2018) have shown that the fundamental nature of the laterally loaded pile problem is three-dimensional, demanding the use of three-dimensional numerical models to properly assess behavior. Previous numerical studies of this nature indicate that such a numerical approach can provide a realistic assessment of pile-soil behavior, thus allowing a rational means for assessing the mechanics at play. This research presents the three-dimensional finite element analysis of a benchmark case history and provides a deformation-based design methodology for the analysis of laterally loaded piles embedded in layered soil. The model is validated with instrumented lateral load tests like those undertaken in the field, enabling an assessment of p-y characteristics that can be applied to their empirical counterparts. It has been expected that the proposed deformation-based methodology would save costs typically expended in field tests.

## 1.6. Organization of Thesis

The thesis has six chapters. The first chapter describes some information on the title and the main task of this work. A literature review would be presented in chapter two. Chapter three labels research methodology. The fourth chapter outlines the different parameters and numerical modeling validation analysis done. Chapter 5 outlines the results and discussion from parametric study. Moreover, chapter six summarizes the work of previous chapters and gives general conclusion and recommendation for possible future work.

# 2. LITERATURE REVIEW

## 2.1. Introduction

Piles have been widely used for supporting axial and lateral loads for a variety of civil engineering structures such as high-rise buildings, transmission lines, bridge piers and port structures. In many cases, lateral loads govern the design of piles.

The analysis of pile under lateral loading is complicated by the fact that the soil reaction is dependent on the pile movement; on the other hand, it is dependent on the soil response. Thus, the problem is one of soil-structure interaction. Introduction of other piles nearby, or in other words consideration of pile group, provides further complexity through pile-soil-pile interaction and the physical repercussions of the group configuration. Additional modification is possible due to construction-related issues such as the installation process, and this is to say nothing of other factors that can affect lateral response, such as the pile head fixity.

In response to these various issues a basic framework of mathematical models supplemented with empirical rules has emerged. Playing a key role has been the understanding of single pile behavior, serving to identify both general pile-soil interaction issues as well as providing a benchmark from which group behavior can be assessed. Single pile behavior will therefore be reviewed in the current section.

Piles have been used to increase the vertical load carrying capacity of foundations for many decades. For the most part, design of pile foundations has been based on empirical formulations and procedures. To date, there has been much research effort focused on the design and behavior of pile foundations to meet increasing needs for efficient and cost-effective construction in more and more unfavorable grounds. Many analytical models that are based on sound engineering principles have been developed in the last two decades. These models generally represent the soil as an elastic medium (H.G.Poulos and E.H.Davis, 1980) or replace the soil with uncoupled, Winkler springs, termed p-y curves. The p-y curve methods have proved to be very versatile and useful as they can be non-linear and have different shapes and form, which had better represent the soil behavior. Unfortunately, due to the high cost of full-scale experiments on piles, soil parameters required for the various models have not been fully calibrated, nor have the models been fully verified yet. Fundamental aspects of soil-pile interaction are still poorly understood.

This chapter serves as a review of the previous studies of laterally loaded pile design, analysis, and construction.

## 2.2. Load Transfer Mechanisms (Statics) of Piles

A proper understanding of the load transfer mechanisms for piles is necessary for analysis and design. Piles transfer axial and lateral loads through different mechanisms. In the case of axial (vertical) loads, piles may be looked upon as axially loaded columns; they transfer loads to the ground by shaft friction and base resistance (Figure 2.1) (Basu et al., 2008). As a pile is loaded axially, it slightly settles and the surrounding soil mass resists the downward movement. Because soil is a frictional material, frictional forces develop at the interface of the pile shaft and the surrounding soil that oppose the downward pile movement. The frictional forces acting all along the pile shaft partly resist the applied axial load and are referred to as shaft resistance, shaft friction, or skin friction. A part of the axial load is transferred to the ground through the bottom of the pile (commonly referred to as the pile base). As a pile tries to move down, the soil mass below the pile base offers compressive resistance to the movement. This mechanism is called base resistance or end-bearing resistance. The total resistance (shaft friction plus end-bearing resistance) keeps a pile in equilibrium with the applied load. Piles that transfer most of the axial load through the base are called end-bearing piles, while those that transfer most of the load through shaft friction are called friction piles. For end-bearing piles, it is necessary to have the pile base inserted into a strong layer of soil (e.g., dense sand, stiff clay, or rock). Typically, engineers would prefer to design end-bearing piles because the base resistance is more reliable than shaft friction. However, if no such strong layer is available at a site, then engineers necessity relies only on shaft friction; in such a case, the pile is called a floating pile.

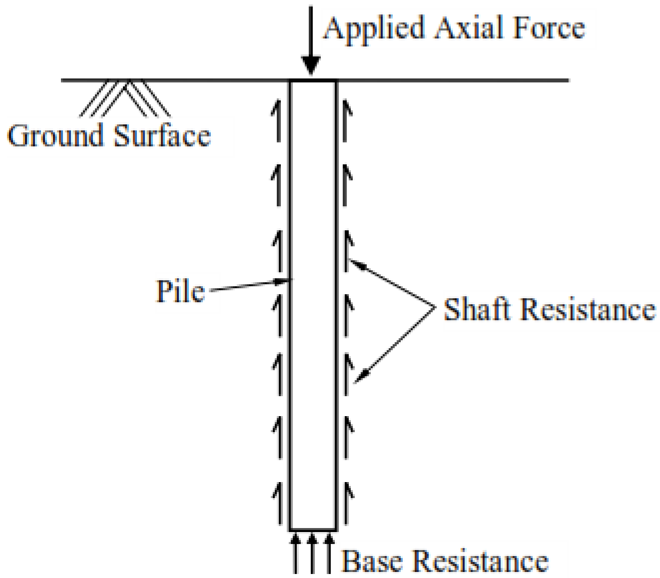


Figure 2.1: Load Transfer Mechanism of Axially Loaded Piles after (Basu et al., 2008)

In the case of lateral loads, piles behave as transversely loaded beams. They transfer lateral load to the surrounding soil mass by using the lateral resistance of soil (Figure 2.2). When a pile is loaded laterally, a part or whole of the pile tries to shift horizontally in the direction of the applied load, causing bending, rotation, or translation of the pile (Fleming et al., 2009) and (Basu et al., 2008). The pile presses against the soil in front of it (i.e., the soil mass lying in the direction of the applied load), generating compressive and shear stresses and strains in the soil that resists the pile movement. This is the primary mechanism of load transfer for lateral loads. The total soil resistance acting over the entire pile shaft balances the external horizontal forces. The soil resistance also allows satisfaction of moment equilibrium of the pile.

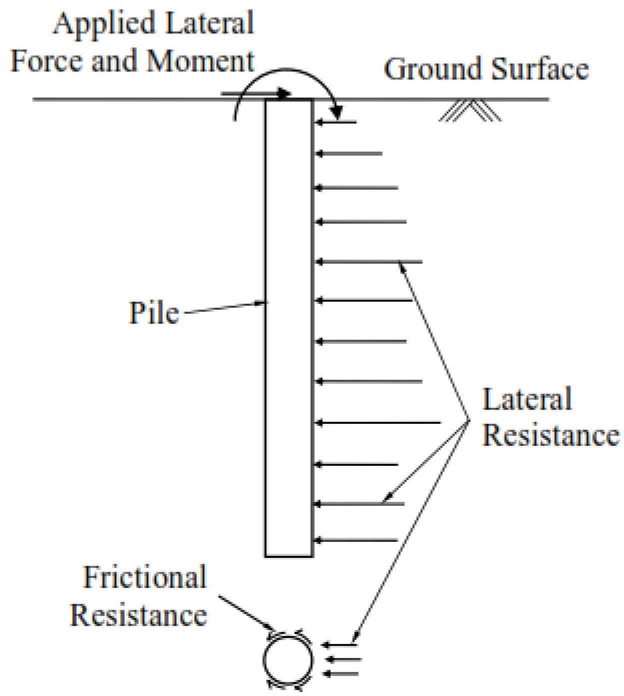


Figure 2.2: Load Transfer Mechanism of Laterally Loaded Piles (Basu et al., 2008)

Often, the load acting on a superstructure is larger than the capacity of a single pile. When that happened, piles are grouped under each column to resist the total force acting at the column base. The piles in a group no longer behave as isolated units but interact with each other and resist the external load in an integrated manner. Consequently, the response of a single pile differs from that of a pile placed within a pile group. Each pile in a group, whether loaded axially or laterally, generates a displacement field of its own around itself. The displacement field of each pile interferes and overlaps with those of the adjacent piles; this results in the interaction between piles.

## 2.3. Kinematics and Failure Modes of Laterally Loaded Piles

The kinematics of axially loaded piles is simple: the pile moves vertically downward under the acting load and, if the resistive forces (i.e., shaft and base resistances) exceed the limit values, then the pile suffers excessive vertical deflection (plunging) leading to collapse. The kinematics and failure mechanisms of laterally loaded piles are more complex and vary depending on the type of pile.

Since laterally loaded piles are transversely loaded, the pile may rotate, bend, or translate (Basu et al., 2008) and (Fleming et al., 2009). As the pile moves in the direction of the applied force, a gap may also open between the back of the pile and the soil over the top few meters. If the pile is short and stubby, it will not bend much but will rotate or even translate (Figure 2.3). Such piles are called rigid piles. If the pile is long and slender, then it bends because of the applied load (Figure 2.4). These piles are called flexible piles. In most practical situations, piles are long enough to behave as flexible piles. For flexible piles, the laterally loaded pile problem is one of soil-structure interaction; i.e., the lateral deflection of the pile depends on the soil resistance, and the resistance of the soil, in turn, depends on the pile deflection.

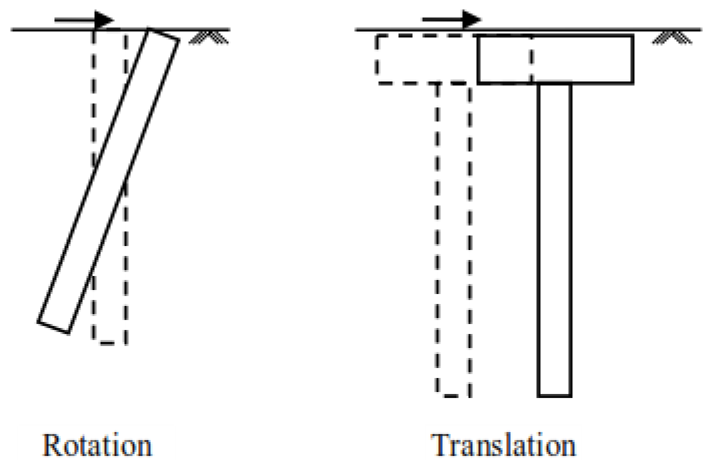


Figure 2.3: Kinematics of Rigid Piles

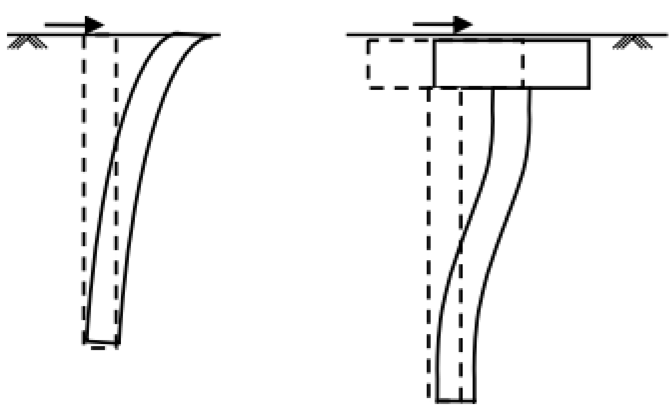

Figure 2.4: Kinematics of Flexible Piles

Failure is a term that engineers define for their convenience. For a structure or a foundation, there is some preset criteria that satisfy for their structural stability and equilibrium. If one or more of those criteria are not satisfied, then the structure or the foundation can be said that it has failed. In general, two classes of criteria: (1) ultimate limit states and (2) serviceability limit states (Basu et al., 2008). Ultimate limit states are associated with dangerous outcomes, such as partial or total collapse of a structure. Serviceability limit states are used as measures to maintain the serviceability of a structure. In general, serviceability limit states refer to tolerable settlements or deflections. For design, all the possible ultimate and serviceability limit states associated with a structural or foundation element are identified and then it is designed so that all the limit states are satisfied.

One ultimate limit state for laterally loaded piles is reached if the resistive stresses in the soil attain the limit (yield) value over a substantial portion of the pile length so that plastic flow occurs within the soil mass resulting in large lateral deflections, translation or rotation of the pile (e.g., inflexible piles, with possible yield or breakage of the pile at one or more cross sections). This ultimate limit state may lead to collapse of the superstructure. For flexible piles, the mechanism consists of a plastic wedge of soil that forms in front of the pile, leading to excessive lateral deflection and bending. If the bending moment is excessive, plastic hinges may form, leading possibly to collapse. Much before this pile-centered ultimate limit state is reached, other ultimate limit states or serviceability limit states may occur as the pile head deflection exceeds the tolerable head deflection. Hence, it is the restriction of the horizontal pile deflection that determines the limits of pile performance and designs in most cases. In fact, in most cases, piles are first designed against ultimate limit states corresponding to axial loads (i.e., against the limit vertical load carrying capacity) and then checked against serviceability limit states corresponding to axial and lateral loads (i.e., against vertical and lateral deflections).

## 2.4. Analysis Methods

Having assessed the statics, kinematics and the possible failure modes of laterally loaded piles, the methods available for analyzing them so that safe designs can be produced are discussed here. Piles with active loading are discussed here. Most of the analyses available in the literature are developed for active loading, although most of the methods can be extended to passive loading as well. Research on analysis of laterally loaded piles started more than five decades ago. Because of such sustained research, a number of analysis methods that can be used for design (an account of the salient analysis methods available can be obtained from (H.G.Poulos and E.H.Davis, 1980), (F.Scott, 1981), (Fleming et al., 2009), (Lymon C.Reese and William F.Van Impe, 2011). Broadly, the methods of analysis can be classified into following approaches:

### 2.4.1. Broms Method (1964a and 1964b)

The Broms method is an approximate approach, which is subject to significant limitations relative to the more sophisticated *p-y* models that are recommended and available using computer software. The Broms method is a simplified limit equilibrium solution that is suitable for simple analyses of relatively short, stiff piles subject to lateral shear and overturning moments. The moment distribution along the length of pile cannot be analyzed from Broms method. Examples of structures that might be analyzed using the Broms method include sign or sound wall foundations in uniform or relatively simple soil profiles.

In order to perform an analysis using this method, a simple soil passive pressure diagram is assumed and a limit equilibrium solution can be obtained through derivation of equations of static equilibrium of shear and moment in the shaft. Although the original paper proposed a method for analysis of piles with full moment connection to a cap which is "fixed" against rotation, it is recommended that the use of the method is limited to these simple applications in which shear and overturning are applied at the top of a shaft which is free to rotate. The method is most suited to analysis of strength limit states. Analysis of deformations (serviceability) in the original papers was based on a simplified subgrade reaction model for an elastic pile hat is not considered very reliable. For analysis of geotechnical strength limit state of a pile using the Broms method, a resistance factor of 0.4 is recommended. This recommendation is provided based on the judgment of the authors, because:

- The method uses a bearing capacity type analysis based on a limit equilibrium solution, like a bearing capacity analysis of a shallow foundation
- The method is recommended only for non-critical structures such as signs, light poles, or sound walls, and not for bridges or retaining walls
- The geotechnical information at specific foundation locations in the type of applications is often sparse, based on crude sampling from borings at widely spaced locations
- The current AASHTO code does not provide guidance for the evaluation of geotechnical strength of piles using the Broms method.

**A. Broms Method for Cohesive Soils**

The maximum soil resistance per unit length of shaft in cohesive soils is taken as 9 times the cohesion (undrained shear strength) times the shaft diameter, with an exclusion zone in the top 1.5 shaft diameters as illustrated on Figure 2.5.

In order to achieve horizontal force and moment equilibrium, the portion of the earth pressure in the upper portion of the shaft will oppose the applied shear force, and the portion of the earth pressure at the base of the diagram will act as shown in order to restrain the shaft toe. The resulting earth pressure, shear, and moment diagrams would be as shown on Figure 2.6.

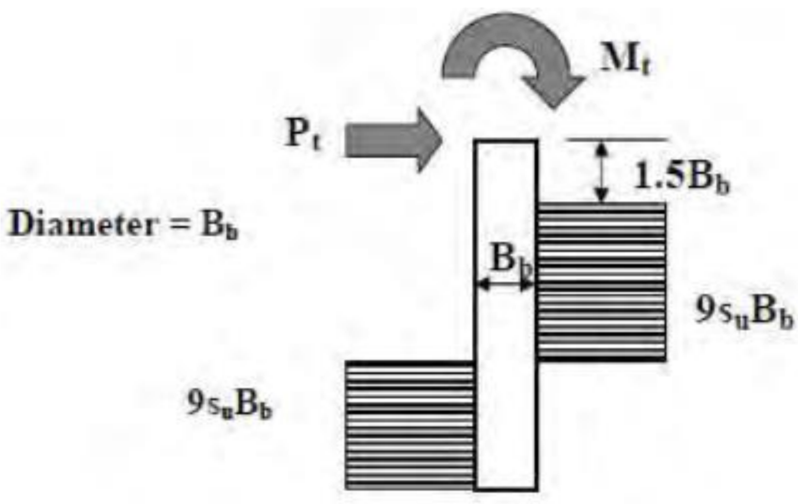


Figure 2.5: Broms Earth Pressures for Cohesive Soils

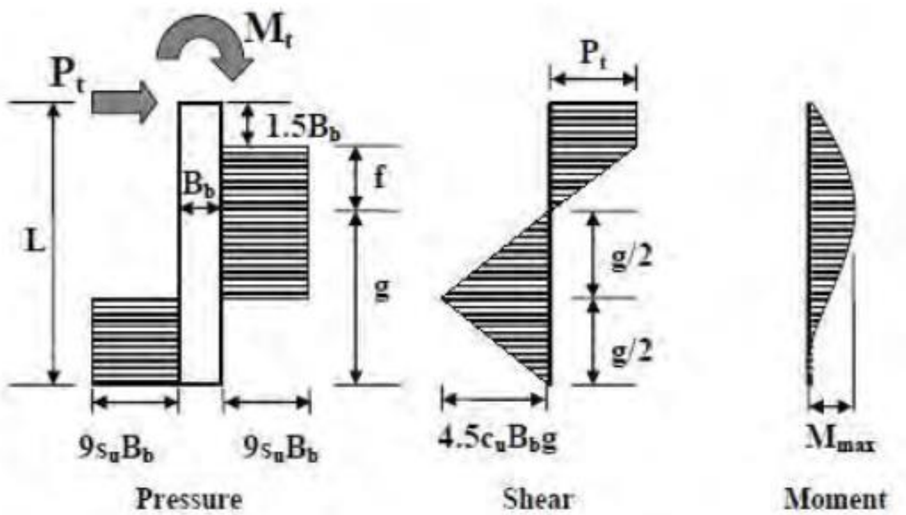


Figure 2.6: Broms Pressure, Shear, Moment Diagrams for Cohesive Soils

The point of zero shear, and thus the point of maximum moment, occurs at a depth, *f*, below the top of the uppermost earth pressure diagram as shown on Figure 2.6. In order to satisfy horizontal force equilibrium about that point, the earth pressures below the point of zero shear must sum to zero, and therefore the earth pressures on each side of the shaft over the region labeled *"g"* must be equally divided on each side of the shaft. The crossover pressures result in the triangular of the shear diagram over this region with the peak at *g/2* as shown. Note that this simplified diagram inherently assumes that the shaft rotates about the point at *g/2* where the earth pressures cross the shaft axis, and that the full earth pressure is mobilized immediately above and below this point even though the displacement must be extremely small near the point of rotation. In order to satisfy moment equilibrium, the resultant moment due to the earth pressures acting on the region *g* below the point of zero shear must equal the maximum moment, which is the moment due to the forces and earth pressures above the point of zero shear.

From the diagrams shown on Figure 2.6, the following equations are obtained:

$P_t = 9S_u B_b f$ ............................................................................................................*Equation 2.1*

Therefore:

$f = \frac{P_t}{9S_u B_b}$ ……………………………………………………………………………….*Equation 2.2*

The maximum moment is given by:

$M_{max} = M_t + P_t(1.5B_b + 0.5f)$ ……………………………………………………………*Equation 2.3*

The maximum moment can also be calculated by applying moment equilibrium at the point of zero shear, or:

$M_{max} = 2.25B_b g^2 S_u$ …………………………………………………………………………*Equation 2.4*

The depth $g$ can be determined as

$g = \left(\frac{M_{max}}{2.25S_u B_b}\right)^{1/2}$ ………………………………………………………………………………*Equation 2.5*

In addition, the minimum pile length can be determined as:

$L \geq 1.5B_b + f + g$.......................................................................................................*Equation 2.6*

### B. Broms Method for Cohesionless Soils

The maximum soil resistance per unit length of shaft in cohesionless soils is assumed to be three times the Rankine passive earth pressure times the shaft diameter. Thus, at a depth, $z$, below the ground surface the soil resistance per unit length of shaft, $p_z$, can be obtained as follows:

$P_z = 3B_b\gamma zK_p = 3B_b\sigma' K_p$ ………………………………………………………………*Equation 2.7*

$K_p = tan^2\left(45 + \frac{\varphi'}{2}\right)$ ………………………………………………………………*Equation 2.8*

Where

$B_b$= the width of the pile/shaft

$\sigma'$ = is the vertical effective stress at depth, $z = z\gamma$

$\gamma$ = unit weight of the soil

$K_p$ = is the Rankine passive earth pressure coefficient

$\varphi'$ = is the effective friction angle of the cohesionless soil.

The earth pressure diagram used for design is illustrated on Figure 2.7. The passive earth pressure should cross the vertical axis at the point of rotation, and the pressures below the point of rotation should act in the same direction as the load. However, as a simplification, the pressure diagram is taken as shown and the portion on the left-hand side is replaced by a concentrated force at the bottom of the shaft (in a manner like the simplified earth support method used for walls). With uniform soil of weight $\gamma$, the vertical stress $\sigma'$ at the base of the shaft at depth $L$ will be $\gamma L$ and the passive earth pressure at the base of the triangular pressure diagram will be $3B_b\gamma LK_p$.

Requirements of overall moment equilibrium are applied in order to determine the minimum length of the shaft, $L_{min}$, to satisfy geotechnical strength requirements. At the base of the shaft:

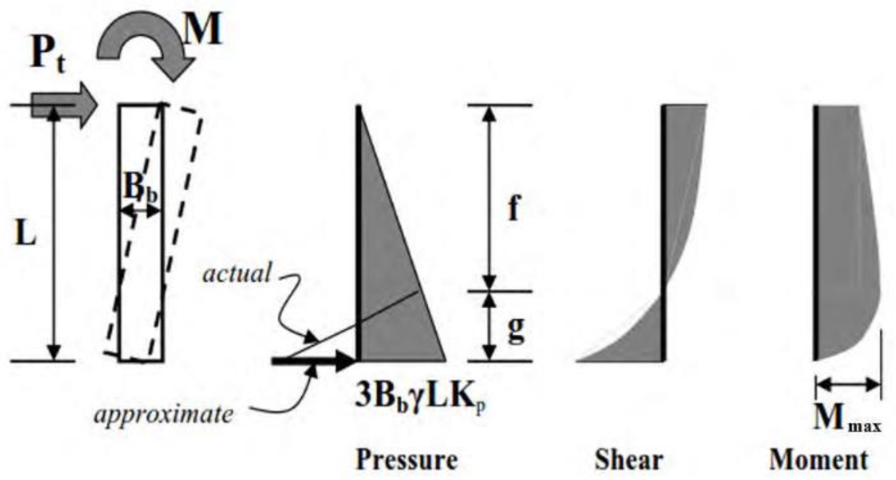


Figure 2.7: Broms Pressure, Shear, Moment Diagrams for Cohesionless Soils

$\sum M_b = 0 = M_t + P_t\, L_{min} - 3B_b\gamma\, L_{min}K_p(\, L_{min}/2)(\, L_{min}/3)$ ……………………. *Equation 2.9*

The solution of the cubic Equation 2.9 provides $L_{min}$.

The point of zero shear, and thus the point of maximum moment, occurs at a depth, $f$ at which point the passive pressure at which point the passive pressure is, $3B_b\gamma f K_p$ so:

$P_t = 3B_b\gamma f K_p \left({f^2}/{2}\right) = 1.5B_b\gamma K_p(f^2)$ ………………………………………………. *Equation 2.10*

$f = \sqrt{\frac{P_t}{1.5\gamma' B_b K_p}}$ …………………………………………………………………………….*Equation 2.11*

The maximum moment,$M_{max}$ is determined from the sum of the moments about depth $f$:

$M_{max} = \sum M_f = M_t + P_t(f) - \left(\frac{B_b\gamma' f^3 K_p}{2}\right)$ ............................................................*Equation 2.12*

Broms provide figures 2.8 and 2.9 for graphical estimate of pile ultimate lateral load capacity for cohesive soil of short rigid pile and long flexible pile respectively.

Figure 2.10 provides the lateral deflection calculation both short and long pile embedded in cohesive soil.

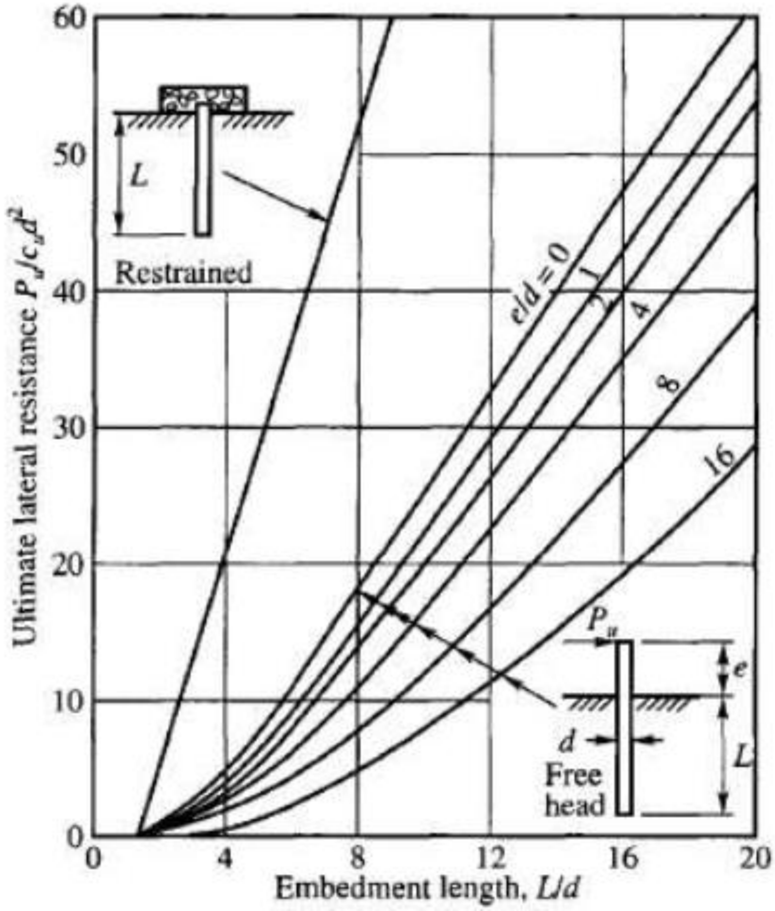


Figure 2.8: Ultimate lateral resistance of short pile in cohesive soil

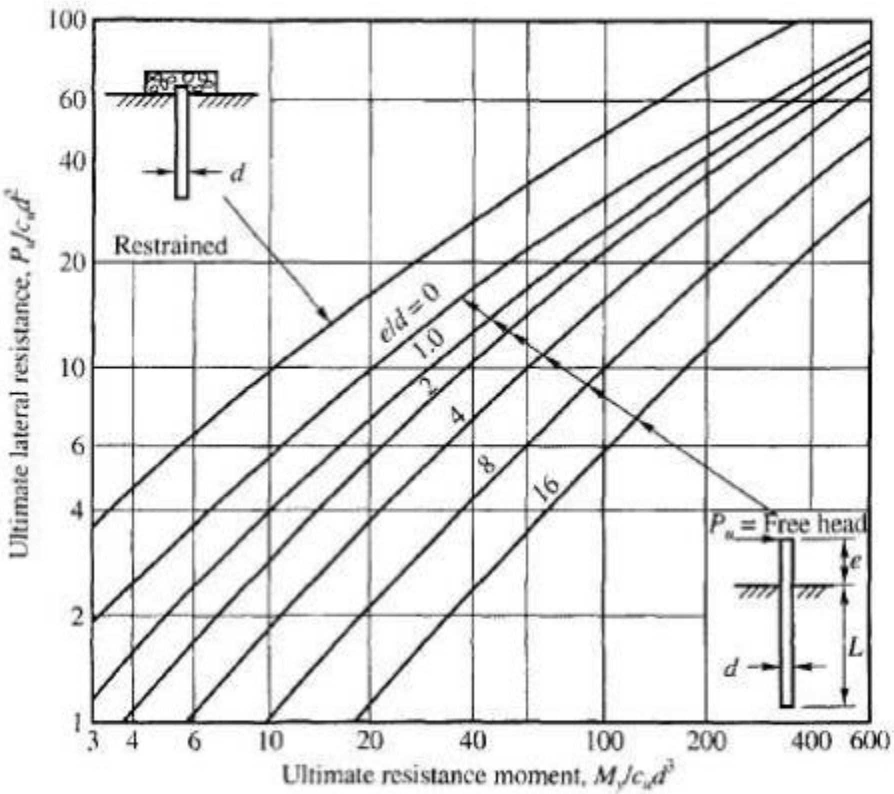


Figure 2.9: Ultimate lateral resistance of long pile in cohesive soil

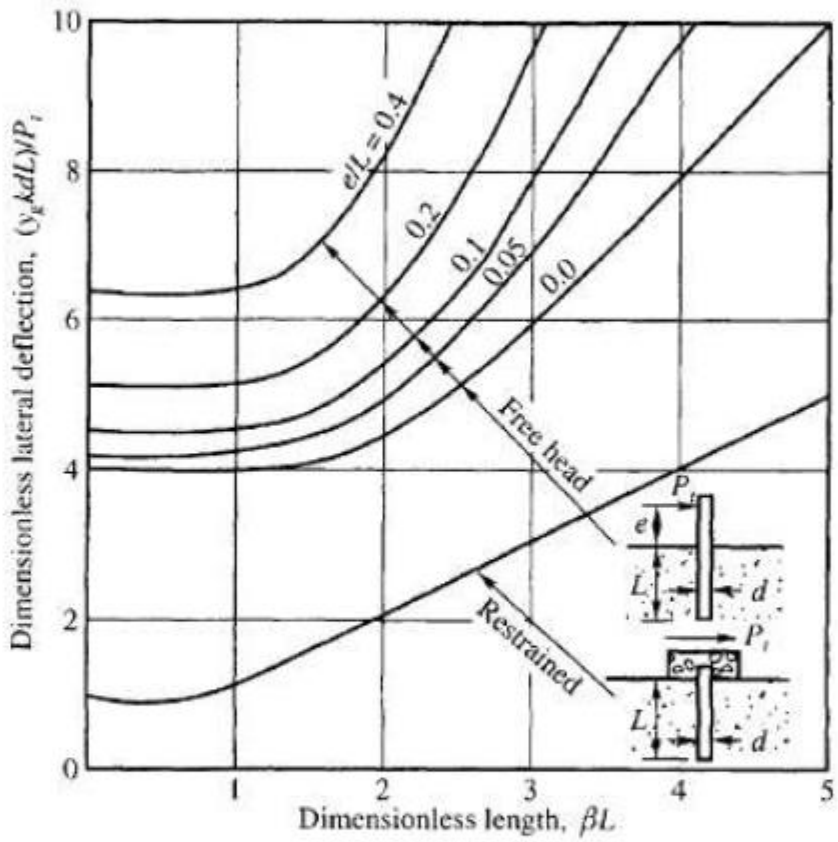


Figure 2.10: Charts for calculation of lateral deflection at ground surface of horizontally loaded pile in cohesive soil (after Broms 1964).

### 2.4.2. Subgrade Reaction Approach

The most traditional method for forecasting pile deflections and bending moments is the Winkler beam method on an elastic foundation, which makes extensive use of the modulus of subgrade reaction. Emil Winkler, who utilized Hooke's law to model the bedding of railway tracks, first articulated the concept in 1867. Winkler modelled the railway track as a continuous beam on an infinite number of disconnected linear-elastic springs that represented the soil. The reaction at any location on the beam is only influenced by the deflection at that same position in this method since it is assumed that the soil bearing pressure is proportional to ground settlement. This approach was later used for laterally loaded piles, since the general behavior is like that of the flexible beams against transverse loads, only rotated at 90°. The mathematical expression for the Winkler method is given by the following equation:

$p = k_h . w$ ………………………………………………………………………………. *Equation 2.13*

Where p = the soil reaction per unit area ($F/L^2$)

$k_h$ = coefficient of sub-grade reaction ($F/L^3$)

$w$ = beam settlement($L$)

The use of reinforced concrete for the foundations and the growing development of the foundation engineering theory in the early 1920s, led to the extension and improvement of the Winkler's hypothesis by using Euler-Bernoulli beam on top of the elastic soil springs (foundation) and apply the loads on the top of beam (Figure 2.11). (M.A.Biot, 1937) and (M.Hetenyi, 1946) developed a fourth order linear differential equation (Eq. 2) that covers the deflection and bending moments for such a beam-foundation system. The input parameters required are the elastic modulus and geometry of the beam, the spring constant of the foundation (soil) and the magnitude and distribution of the applied load. Because of the analysis, the beam deflection, bending moment and shear force along the span of the beam can be determined.

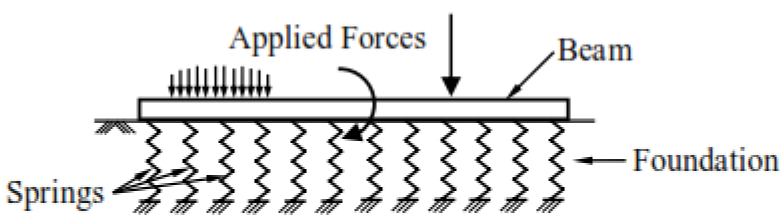


Figure 2.11: A Beam on an Elastic Foundation (after Ermi Winkler)

$E_p I_p \frac{d^4u}{dz^4} + Q \frac{d^2u}{dz^2} + k_h uD = 0$ …………………………………………………………….*Equation 2.14*

Where $u$ = Lateral deflection of pile at point along the $z$ length of the pile

$E_p$ = Pile modulus of elasticity

$k_h$ = horizontal coefficient of subgrade reaction

$P$ = Soil pressure over the pile

$D$ = Pile diameter

$I_p$ = Pile cross section moment of Inertia

$Q$ = Axial load on pile

Other researchers presented work accounting for the variation of $k_h$ with depth. For instance, (E.Barber, p. 1953) proposed solution to calculate the deflections and rotations at the ground surface when $k_h$ is increasing linearly with depth. (Terzaghi, 1955) Proposed rules for the selection of the recommended values of $k_h$ that can be used in Eq.2.14 for over consolidated clays, stiff clays, and sandy soils. However, no experimental data or analytical procedure was given to validate his recommendations. (Lymon C. Reese and Hudson Matlock, 1956) Obtained non dimensional charts to be used in calculating the ground-line deflection, slope, shear, and maximum bending moment on the pile and modified Eq.2.13 for laterally loaded piles. This method was based on p-y curves (Eq. 2.15) that are manually created in addition to manual numerical solutions.

Idealizing the soil foundation as a Winkler foundation consisting of a bed of infinitely closely spaced, independent springs each possessing a linear vertical pressure $q$ per unit area versus vertical deflection *w* relationship as follows,

$\frac{q}{w} = k_o \;\; or \;\; \frac{qb}{w} = k$ …………………………………………………………………….*Equation 2.15*

Where: $k_o$ = subgrade modulus soil ($FL^{-3}$ dimensions)

$b$ = width of beam

$k = k_o b$ = subgrade modulus for soil ($FL^{-2}$ dimensions)

The general differential equation governing the deflected shape of a beam resting on a Winkler medium is:

$E_b I_b \frac{d^4 w}{dx^4} + kw(x) = p(x)$ ..........................................................................*Equation 2.16*

The general solution of Equation (2.16) is given by:

$w = (C_1 \cos \lambda x + C_2 \sin \lambda x)e^{\lambda x} + (C_3 \cos \lambda x + C_4 \sin \lambda x)e^{-\lambda x}$ ……………………*Equation 2.17*

Where $C_1$ through $C_4$ are constants, and

$\lambda = \sqrt[4]{\frac{k}{4EI}}$ *($L^{-1}$ dimensions)*…………………………………………………………………*Equation 2.18*

Consider now a beam of infinite length subjected to a concentrated force, P, from the boundary conditions; Equation 2.17 becomes,

$w = (C_3 \cos \lambda x + C_4 \sin \lambda x)e^{-\lambda x}$ ..........................................................................*Equation 2.19*

In equation 2.19, for the left side of the beam $w(-x) = w(x)$ (M.Hetenyi, 1946) .

The parameter λ is dependent on the properties of both the soil and beam, and its reciprocal represents a characteristic length of the soil-beam system. If the beam is very stiff compared with the soil then the characteristic length is large, and a load applied to the beam will cause vertical deflections of the soil for a considerable distance from the point of load application. Conversely, a beam that is very soft compared with the soil (i.e., a very stiff soil) will result in a small characteristic length and only cause vertical deflections in the immediate vicinity of the point load (F.Scott, 1981). Although use of subgrade reaction theory to depict soil is far removed from real soil behavior, identification of λ as an interactive measure dependent on the relative stiffness of the soil and structure, and in turn the dependency of behavior on such a measure, is a fundamental aspect of soil structure interaction.

In the context of laterally loaded piles, the dependence of behavior on relative stiffness has resulted in the need to distinguish between “short” (rigid) and “long” (flexible) piles. These definitions acknowledge a somewhat intuitive sense of pile behavior whereby a very short and relatively stiff pile (e.g., a fence strainer-post) would be expected to deflect in a rigid manner when laterally loaded. Whereas a very long pile in the same situation would be expected to exhibit a different type of behavior due to the increased embedment and accompanying fixity that this implies. (C.Reese, 1986) discussed this dependence of lateral behavior on pile length, noting that short piles can deflect a large amount at the ground line given movement of the pile tip, but with increasing depth of penetration the soil resistance at the pile tip increases until a point is reached at which ground line deflection reaches a limiting value. This type of behavior is depicted in Figure 2.12, for the case of both lateral load (Pt) and moment (Mt) applied at the ground line, assuming an elastic ($E_pI_p$) pile model and constant horizontal subgrade modulus ($k_h$) soil model. As shown, a so-called “critical length” $L_c$ exists, beyond which any additional pile length has no further influence on the pile head response.

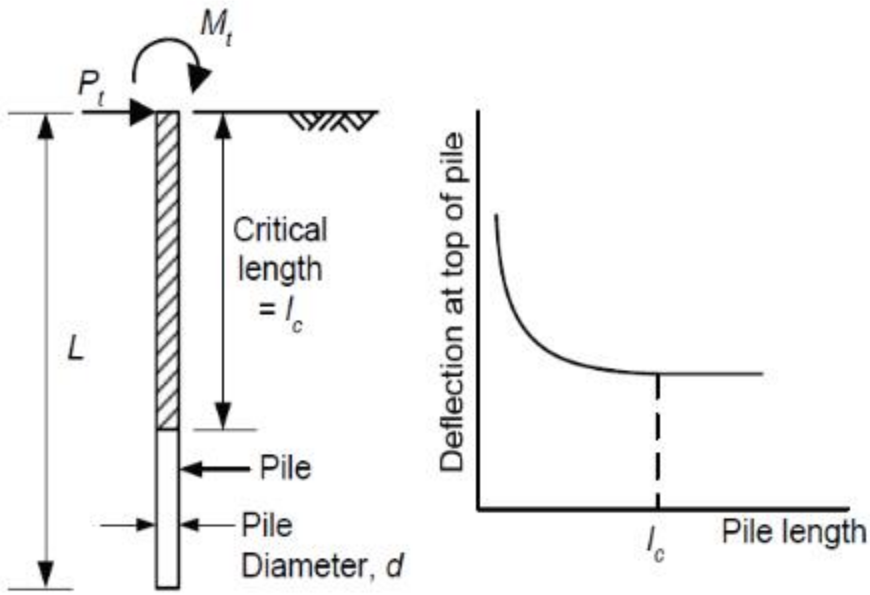


Figure 2.12: Critical length for a laterally loaded pile after (Lymon C.Reese and William F.Van Impe, 2011).

Thus, a flexible pile is defined as a pile whose length equals or exceeds its critical length. In subgrade reaction terms, such critical lengths have been established for the case of a horizontal subgrade modulus ($k_h$) that is constant with depth (as in Figure 2.12), in which case:

$L_c = \frac{4}{\lambda}$ ……………………………………………………………………………….*Equation 2.20*

Where: $\lambda = \sqrt[4]{\frac{k_h}{4E_pI_p}}$

$k_h$ = Subgrade modulus for soil ($FL^{-2}$ dimensions)

$E_p$ = Young's modulus for pile

$I_p$ = Second moment of area for pile

Moreover, for the case of a horizontal subgrade modulus increasing linearly with depth, in which case:

$L_c = 4T$ ……………………………………………………………………………….*Equation 2.21*

Where: $T = \sqrt[5]{\frac{E_pI_p}{n_h}}$

$n_h$ = constant of horizontal subgrade reaction ($FL^{-3}$ dimensions), given

$k_h = n_h z$ ($FL^{-2}$ Dimensions), where z is the depth

While these critical length values are subject to the limitations inherent in idealizing the pile-soil system in such a simplistic way, the concept of a critical length is nevertheless of general validity and acknowledges the dependence of lateral behavior on a certain mobilized depth of soil that may or may not extend the entire length of the pile. As a comment aside, this physical attribute of lateral behavior is also suggestive of some form of normalization, an early example of which was the non-dimensional linear solutions derived by (H.Matlock and L.C.Reese, 1960) using principles of dimensional analysis.

(H.G. Poulos and T.S. Hull, 1989) Method, a linear elastic soil response due to lateral pile movements was assumed. A critical length, $L_c$ equation (2.22), exists for a laterally loaded pile, over which any increase in pile length has no influence on the pile head deflection. The critical pile length $L_c$ is a function of the relative stiffness of pile and soil. For uniform soil, $L_c$ can be calculated from the following equations:

$L_c = 4.44(\frac{E_p I_p}{E_s})^{0.25}$ .........................................................................................*Equation 2.22*

Where: $E_p I_p$ = pile rigidity

$E_s$ = Soil Young's modulus of elasticity

Given that there were potentially simple answers, it was reasonable that subgrade reaction theory was initially preferred to evaluate lateral pile-soil interaction; however, choosing the right subgrade modulus posed significant challenges. (Terzaghi, 1955) addressed this worry in the now-classic study that serves as a reminder of the fundamental constraints associated with subgrade reaction theory as well as the challenge of determining an adequate value for the subgrade modulus. Terzaghi made the crucial statement that the theory was only roughly valid for pile-soil contact pressures lower than approximately half the ultimate bearing capacity of the soil under lateral load. The writer also emphasized the significance of the pile's dimensions and the type of soil. These issues were considered where constant, linearly increasing subgrade reaction models idealized stiff (over consolidated) clay, and sand subgrade characteristics, respectively. Pile dimensions were addressed using the idea of different horizontal pressure bulbs mobilized by different pile widths.

These simple ideas underlined the need to appreciate both the different deformation characteristics of soils, and possible effects of size due to differing volumes of the surrounding soil mass being affected by different loaded areas. The issue of flexural rigidity of a structure, such as a pile, and its effect on the subgrade modulus was only briefly mentioned by (Terzaghi, 1955), and only then in the context of theoretical work.

(P.W. Rowe, 1956), on the other hand, specifically pursued the response of a laterally loaded single pile in real sand and noted significant differences in the back-calculated values of subgrade modulus depending on whether the pile was rigid or flexible. Though weakened somewhat by use of some data from scaled-down 1-g laboratory pile-soil models and thus subject to scaling errors, this work by Rowe was of value given that it utilized subgrade reaction theory in conjunction with experimentally observed data. In doing so, it served to demonstrate the highly variable nature of the subgrade modulus during lateral loading because of the actual nonlinear interplay between pile and soil. This resulted in a rather convoluted analysis procedure, relying on various assumptions and approximations in order to adapt the underlying subgrade reaction theory to agree with observed behavior.

That subgrade reaction theory is limited from both a physical and theoretical point of view is a fact that has long been recognized: Terzaghi himself expressed reservations in publishing his 1955 paper and only did so after numerous requests (C.Reese, 1986). (M.Jamiolkowski and A.Garassino, 1977) acknowledged this limitation in their review of soil moduli for laterally loaded piles, noting the important observation made earlier by (B .McClelland and J. A. Jr.Focht, 1958a) that the subgrade modulus is not a property exclusively of the soil, but simply a convenient mathematical parameter that expresses the ratio of soil reaction to pile deflection. In doing so, such a parameter depends on the characteristics of the pile (i.e., pile geometry, flexural rigidity, boundary conditions at the top and bottom of the pile, etc.), the soil, and the way the pile and soil characteristics change with the level of lateral loading applied.

In response to this complex state of affairs, two general categories of design approaches for single piles have emerged: a) Those that retain the basic qualities of subgrade reaction theory in the form of discrete, nonlinear load-transfer mechanisms along the pile length depicting the soil reaction to pile deflection relationship; and b) those that represent the soil as a continuum.

Here, the Discrete Load-Transfer and Continuum techniques will be used to refer to the two methods. However, limit equilibrium approaches must also be mentioned before talking about these strategies, as demonstrated by Broms' work. This method, which is a limit analysis, is limited to ultimate (failure) conditions where it is possible to make fair assumptions about the lateral soil pressures and easily find solutions by using the statics equations. A brief description of Broms' work will be given even though it is largely superfluous now given the adaptability and capabilities of the continuum and discrete load-transfer approaches. The work provides an instructive account of lateral soil-pile interaction and is a suitable precursor to the more sophisticated continuum and discrete load-transfer approaches.

### 2.4.3. Continuum Method

In the continuum approach, the assumption of modeling the soil by linear or nonlinear springs is replaced by a more appealing and realistic representation. The soil is represented by an infinite, linear and elastic medium and its behavior is described by the deflection along the vertical soil profile, (Kavitha et al., 2016). However, this approach is hard to be used by the engineers in practice due to its mathematical complication. The works in this field and they are grouped in two main categories: (a) the boundary element method (BEM), and (b) the simplified continuum models.

#### A. Boundary Element Method (BEM)

The early work on BEM for laterally loaded piles goes back to (D.Douglas and E.Davis, 1964) who introduced a simple theory for a laterally applied load and a moment on the top of a thin vertical plate buried in elastic media. The mathematical theory for the proposed method included two steps: (a) the integration of the (R.D.Mindlin, 1936) equation for a horizontal displacement induced by a lateral point load within a semi-infinite mass, and (b) the calculation of the distributed normal stress by employing a numerical solution. In addition, it was assumed that the plate is perfectly smooth and the adhesion between the plate and the soil is neglected. Similarly, (W.R.Spillers and R.D.Stoll, 1964) proposed a simplified theoretical solution based on BEM by introducing a limiting lateral pressure value for the soil-pile interaction to account for the soil nonlinearity for a pile in both elastic half-space and plastic half space.

(H.G.Poulos, 1971a,b), utilized the previous work and contributed significantly in this field. The author introduced the stress for single and group pile-soil system using the BEM with various boundary conditions at the top and bottom of the pile. The pile was modelled as a thin rectangular strip, which interacted with an ideal linearly elastic media. As shown in Fig. 2.15, the pile was divided into equal segment lengths, except at the top and bottom of the pile. The response of the soil-pile interaction system was calculated by considering an applied normal uniformly distributed load on each pile segment, whereas, the shear stress at the interface of the pile sides was neglected. Further, the horizontal displacement at each segment can be calculated by equating the displacements of the pile and soil at the center of each segment. In this process, the soil horizontal displacement was calculated through the (R.D.Mindlin, 1936) equation, while the pile deflection was calculated by the differential equation, which is expressed as a finite difference expression for bending of a thin beam. (H.G.Poulos, 1973), had improved his model by considering the soil yielding and nonlinearity, i.e. the elastic-perfectly plastic soil behavior.

Moreover, (P.K.Banerjee and T.G Davis, 1978) used the BEM to analyze the laterally loaded piles in a two-layered elastic half space system with soil modulus that is linearly increasing with depth. The results of the proposed theory were compared with the behavior from full-scale tests; they showed that their method could provide a more rigorous prediction of the response, due to the linear variation of soil modulus. Thereafter, (T.Davies and M.Budhu, 1986), (M.Budhu and T.G.Davies, 1987,1988) extended the linear algorithm of (P.K.Banerjee and T.G Davis, 1978) to account for the nonlinear behavior of laterally loaded piles embedded in over consolidated clays, cohesionless soils and soft clays. The soils were modelled as linear elastic at small strains, while the soil plastic behavior was considered when the soil pressure at the pile surface was equal to certain values.

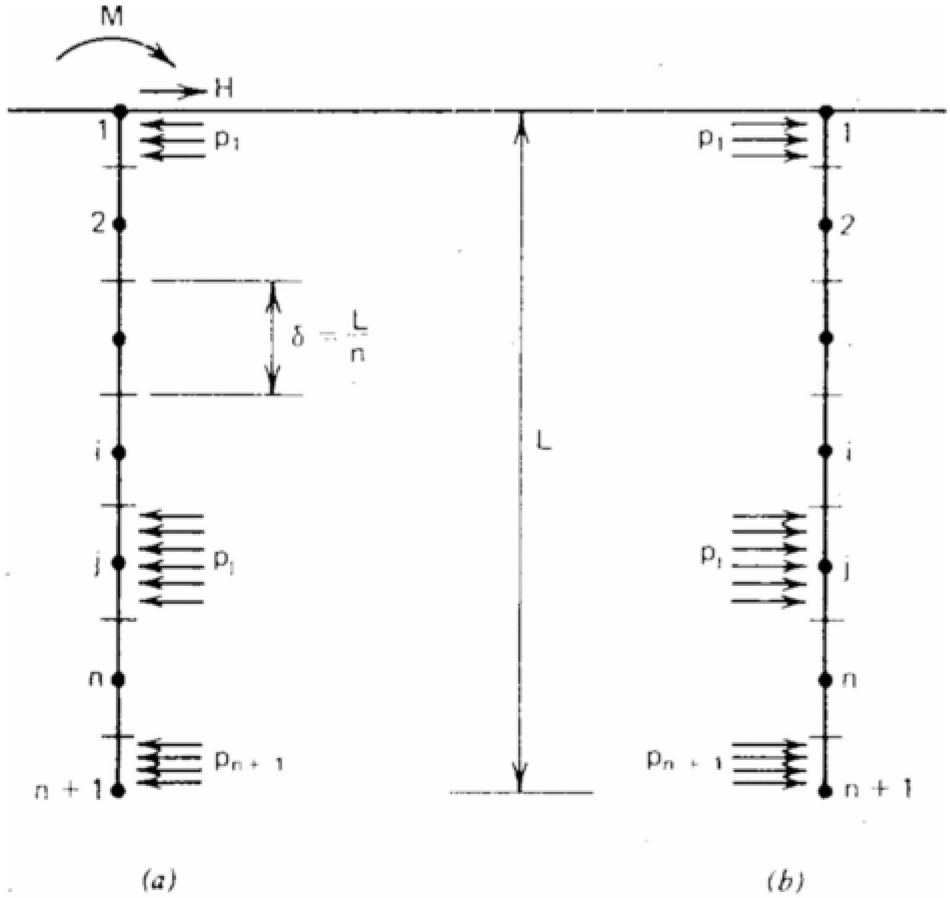


Figure 2.13: Schematic diagram of (H.G.Poulos and E.H.Davis, 1980) method

**B. Finite Element Method (FEM)**

The FEM method is a mathematical technique used to calculate an approximate solution to the partial differential equations based on the continuum theory (C.Desai and G.Appel, 1976) started the early work on the 3D FEM by proposing a general finite element procedure to study the behavior of laterally loaded piles and their interaction with the soil. The soil behavior was assumed to be linear-elastic and the pile was modelled as a 1-D beam element. The interaction between the pile and the soil was modelled using a thin-layer element, which was capable to consider different modes of deformations, e.g. stick mode, gapping, or slippage. It was found that the use of the interface element considerably affected the pile-head displacements. (M.Faruque and C.Desai, 1982) Included the material and geometric nonlinearity in their 3D finite element model for axially and laterally loaded piles. The soil nonlinear stress-strain relation was modelled with the Drucker

Prager plasticity theory. The authors concluded that the geometric nonlinearity had a significant effect on the analysis of pile-soil interaction.

(D.A.Brown, M. Kumar,et al., 1989) Developed p-y curves by creating 3D finite element models in ABAQUS considering elasto-plastic behavior for the soil. The p-y curves and the field results were not in a good agreement due to the simplicity of the soil model. However, (D.A. Brown and C.F. Shie, 1990, 1991), concluded that the 3D finite element models are an effective tool to capture the 3D the interaction between the piles and the soil, the soil nonlinearity, the variation of the soil strength with depth, and the interface friction. The model for the interface frictional element accounted for two soil constitutive laws, i.e. a simple elastic-plastic model with a Von Mises yield surface and an extended Drucker-Prager model with non-associated flow. The p-y curves were in good agreement with those obtained from the COM624 program. Additionally, the authors recommended the FEM for the evaluation of the factors influencing the behavior of the laterally loaded piles.

(Trochanis et al., 1991), who studied the nonlinearity in pile-soil interaction for axially and laterally loaded piles, presented another important work. Their soil constitutive models included a linear elastic and a Drucker–Prager model. The pile was modelled as a 1-D beam element and a special 2-D interface element was used to capture the pile-soil interaction. The interface element was characterized by a friction coefficient, its geometry, and an elastic stiffness. The main findings of this study were the factors that affect significantly the axially and laterally loaded piles, which are the interface slippage and gap formation, respectively.

Additional work on FEA was presented by (Z.Yang and B.Jeremi, 2005). They studied the effect of layered soils on the behavior of laterally loaded piles and provided accurate p-y curves. A simple von Mises material model and a Drucker–Prager model respectively modeled the clay and sandy soils. In addition, the pile-soil interaction was simulated using a thin layer element. The authors concluded that a simple elastic-plastic soil model could predict the pile head deflection with reasonable accuracy. Moreover, it was found that the upper soil layers influence the lower layers and vice versa, in addition to the antisymmetric effect of layered soils.

(K.Yang and R.Liang, 2006) , investigated the effect of the push-pull resistance for laterally loaded drilled shafts in rocks using a 3D finite model. The modified Drucker-Prager model was used for the modelling of the soil, while the piles were modeled as an elastic material. The interaction behavior was simulated with a surface-based contact element, where the master and slave surfaces were the shaft surface and rock surfaces, respectively. The results from the 3D model showed the insignificance of the pull-push resistance compared to the resistance to the applied moments at the ground surface, which is less than 5%.

(M.Ahmadi and S.Ahmari, 2009), created a 3D finite element model to study the effect of the shear strength anisotropy and the soil mass secondary structure on laterally loaded piles. The results of two full-scale case studies were considered in their analysis. Matlock reported the first case study referring to a steel pipe in soft clay and Reese and Welch reported the second case study for a cast-in-place pile in over consolidated clay. The maximum moment and moment distribution of the analyses were compared to the field results. The soil model considered the von Mises constitutive law, which did not consider the effect of soil anisotropy. Therefore, the soil shear strength and modulus of elasticity had to be back calculated by fitting the pile head load-deflection curve to the field results. The back-calculated shear strength was used as an input to the proposed model to predict the pile-head load vs maximum moment and moment distribution curves. Then a comparison was made between the measured and the predicted curves. The p-y curves from the model were compared to the two p-y curves proposed by Matlock and Wu et al. A sensitivity analysis was carried out using the ANSYS software to study the model dimensions, mesh fineness, contact stiffness, and pile-soil adhesion. It was concluded that using back calculated shear strength and modulus of elasticity provided a good correspondence between the finite element analysis and the field measurements.

(Peng et al., 2010), investigated the effect of fin dimensions on the lateral capacity of the pile in sand. The Mohr-Coulomb constitutive model was used in the numerical analysis using the software PLAXIS-3D. The sand was assumed a linear elastic perfectly plastic and the soil Young's modulus was assumed to increase linearly. The ultimate load was defined when the slope of the p-y curve was less than 0.05 MN/m, i.e. when the curve was straight and the pile failure load was taken as the displacement equal to 10% of the pile diameter. The numerical analysis results were compared to laboratory test results (1-G model tests) for verification purposes. The conclusions were:

1. The lateral resistance increased when the length of the fins increased
2. Fins placed near the pile head provided more resistance than those near the pile tip

3. The lateral resistance varied with the direction of loading in relation to the direction of the fins but the difference was acceptably small for design purposes making the direction of the piles immaterial

(Mardfekri et al., 2013) assessed the existing simplified methods (e.g., beam on elastic foundation, p-y method, and SALLOP) for predicting the deflection of laterally loaded piles in clay and sand by using linear and nonlinear FE analyses. The first objective was to compare the results of different analysis methods for laterally loaded piles and illustrate the variation of the results. The second objective was to show the effect of the pile diameter on the accuracy of the simplified methods. Three pile diameters (1m, 2m and 4m) were presented in the paper. Four different models using linear analysis were created and the influence of the pile diameter was investigated. These models were:

1. A 3D ABAQUS finite element model
2. A model in which the soil was reproduced with 3D elements and the pile with 1-D beam-column elements
3. A model using a consistent boundary matrix
4. A Winkler foundation model

In addition, three models were used for the case of nonlinear analysis as follows:

1. The same 3D ABAQUS finite element model of the previous runs. However, the soil and pile-soil interaction were nonlinear
2. A model using the p-y curves (sand, hard clay p-y curves by Reese)
3. A model implementing the simple SALLOP approach

The results of linear analysis showed that the pile head deflection is not only a function of EI but also a function of the pile diameter. Furthermore, modeling the pile as 1-D beam-column element leads to a smaller contribution of the surrounding soil to the lateral stiffness of the pile. Comparing the nonlinear results from the 3D ABAQUS finite element model to the results of the other two models, it is found that both the p-y model for sand and the SALLOP approach, provide reasonable results for the pile of 4m in diameter. However, the accuracy deteriorates for smaller diameter piles. Further, the p-y curve model for clay as well as the SALLOP provide reasonable results for the pile of 1 m diameter but deteriorate for the piles of larger diameters.

(Tuladhar et al., 2013) investigated the potential of 3D finite element models in simulating pile-soil interaction using the findings of full-scale field testing as the basis. 20-node solid elements were used to model the soil. The piles were either modelled as 20-node solid elements or as 3-node fiber-based beam elements. In comparison to the field data, the model FB-Mon1 significantly underestimated the pile's lateral load capacity since it neglected to account for pile volume. The precision was acceptable when a rough mesh was used, though. The stiffness reduction factor was not considered in the SL-Rev1 model, which resulted in an overestimation of the pile's lateral load capacity. When 0.2 stiffness decrease was considered in model SL-Rev2, the load displacement curves and field data were in good agreement.

## 2.5. Ultimate Lateral Resistance

Structures on pile foundations may be subjected to lateral forces and movements because of ship impact and wave action in harbor and offshore structures, retaining walls, high wind forces in transmission-tower foundations, and lateral accelerations acting on structures in earthquake zones. Therefore, one key issue for pile design may be estimation of the ultimate lateral resistance. Various methods have been proposed to estimate the ultimate lateral load capacity Hu ( (B.Hansen, 1961), (B.B.Broms, 1965).

One of the most popular methods for estimating Hu is Broms' method (Lee et al., 2010). For unrestrained or free-headed piles, (B.B.Broms, 1965) assumed that the ultimate soil resistance is equal to three times the passive Rankine earth pressure (H.G.Poulos and E.H.Davis, 1980).

There are many different definitions regarding the ultimate pile capacity either from deflection or from load point view. It can be determined based on the excessive lateral displacement of the pile head or the rotation of the pile (Hu, et al. 2006). According to (Sawwaf, 2006), the ultimate lateral capacities can be defined as the loads corresponding to the lateral displacements at the pile head equal to around 10% of the diameter of the pile. As stated by (E.A.Dickin and R.B.Nazir, 1999), it can also be obtained from the p-y curve as the point where the curve turns into linear or considerably linear. It can also be defined as the maximum load from the p-y curve when the load cannot be increased with deflection. In the Helmer’s field test in Virginia, in order to avoid additional deflection, loading has been terminated once the tests reached desired deflections.

A horizontal load test was carried out on a pile consists of placing two piles at some distance from each other and either pulling them toward each other or pushing them apart. The resulting load displacement curve for one pile gives the horizontal load *Ho* versus the horizontal displacement $y_o$ (Figure 2.14). From this curve, an ultimate load *Hou* can be defined as the horizontal load Ho corresponding to a displacement equal to one-tenth of the pile diameter (B/10) (Briaud, 2013).

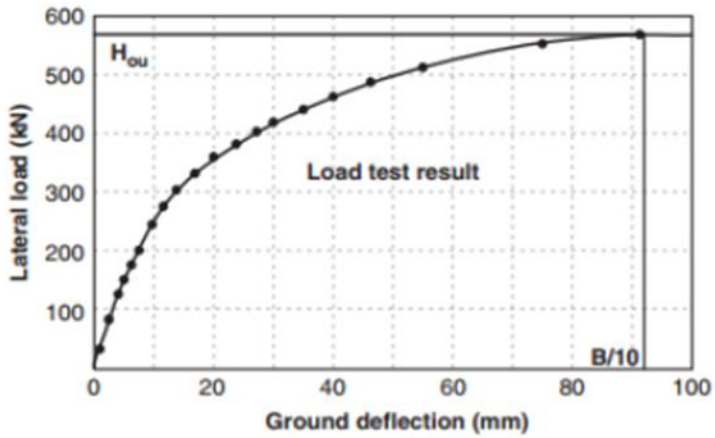


Figure 2.14: Load test result (Briaud, 2013)

In addition, in finite element method the control factor in evaluating the ultimate lateral load capacity of the piles is the yield of the maximum allowed lateral displacement at the pile head, which is taken to be 10% of the pile diameter as it, is more compliant with the design criterion (ASTM STP-835, 1983 and USACE, 1998).

According to British Standard as recommended in BS EN 1997-1:2004+A1:2013, 7.6.1.1(3), the ultimate horizontal load measured at deflection equal to 10% of the pile's diameter when it is difficult to define the ultimate limit state from the loading deflection curve.

## 2.6. Constitutive Models

Soil is a complicated material that behaves non-linearly and often shows anisotropic and time dependent behavior when subjected to stresses. Generally, soil behaves differently in primary loading, unloading, and reloading. It exhibits non-linear behavior well below the failure condition with stress dependent stiffness. Soil undergoes plastic deformation, is inconsistent in dilatancy, and experiences small strain stiffness at very low strains and upon stress reversal. In addition to soil behavior, its failure in three-dimensional state of stress is extremely complicated. Numerous criteria have been devised to explain the condition for failure of a material under such loading state.

Currently, various constitutive models for the soil have been developed. These models cover a wide range of soil features such as anisotropy, cyclic loading, creep etc. The selection of a constitutive model for a geotechnical application depends on the mechanical properties of the soil. (i.e. permeability, stiffness and strength), previous history on the mechanical properties of the soil and the stress changes that will occur in feature (M.Wood, 1990).

In the finite element analysis, reliable predictions can be achieved by using an appropriate constitutive model for a geotechnical problem. In general, the criterion for the soil model evaluation should always be a balance between the requirements from the continuum mechanics aspect, the requirements of realistic representation of soil behavior from the laboratory testing aspect, convenience of parameter derivation and simplicity in computational application. The application of some constitutive models in Plaxis finite element model is briefly discussed below used for this study.

### 2.6.1. Linear Elastic Model

The use of the linear elastic model is quite common to model massive structures in the soil or bedrock layers that include piles and so on (R.B.J. Brinkgreve and W. Broere, 2006). This model represents Hooke's law of isotropic linear elasticity used for modelling the stress–strain relationship of the pile material. Linear elastic constitutive model is probably the most common model used to approximate the stress-strain relationship of materials. Linear elastic models involve two elastic stiffness parameters namely Young's modulus (E) and Poisson's ratio (ν). The linear elastic model is not suitable to model soil because soil behavior is highly nonlinear and irreversible, but it is appropriate to model stiff volumes in soil like concrete structures.

### 2.6.2. Mohr Coulomb Model

The Mohr Coulomb Model is a linear elastic and perfectly plastic model. It involves five parameters, both elastic and plastic behavior parameters i.e. Young's modulus (E) and Poisson's ratio (v) for soil elasticity, friction angle (ϕ) and cohesion(c), for soil plasticity and the dilatancy angle (ψ).

The stiffness behavior below the failure line is assumed to be linear elastic according to Hook's law. Hence, the model does not accurately predict deformation behavior before failure, especially in situation where the stress levels are changing or multiple different stresses paths are allowed. However, the model does not show softening behavior after peak strength. Soft soils like normally consolidated clays, generally show a decreasing mean effective stress during undrained shearing, whereas the Mohr-Coulomb's model would predict a constant mean effective stress in this case, which results in an over prediction of the shear strength (Plaxis 3D Foundation Manual,2006).

The soil in the problems of this paper is modeled as elasto-plastic material. The basic principle of elasto-plasticity is that strains and strain rates are decomposed into an elastic part and plastic part as shown in Figure 2.15.

Hooke's law is used to relate the stress rates to the elastic strain rates. According to the classical theory of plasticity, plastic strain rates are proportional to the derivative of the yield function with respect to the stresses. This means that the plastic strain rates can be represented as vectors perpendicular to the yield surface. This classical form of the theory is referred to as associated plasticity. However, for Mohr-Coulomb type yield functions, the theory of associated plasticity overestimates dilatancy (Plaxis 3D Foundation Manual, 2006).

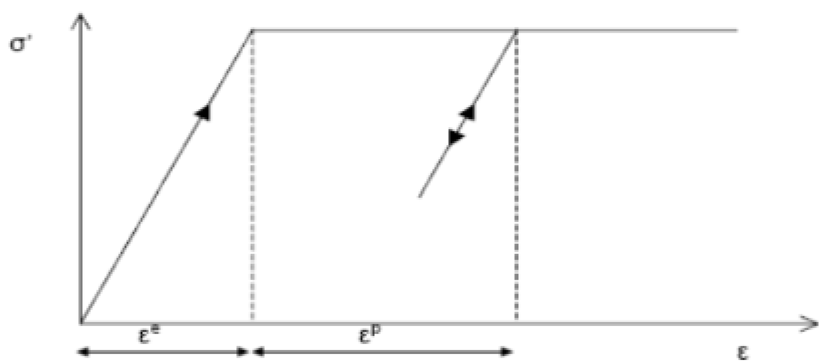


Figure 2.15: Basic idea of an elastic perfectly plastic model (R.B.J. Brinkgreve and W. Broere, 2006)

The Mohr-Coulomb yield condition is an extension of Coulomb's friction law to general states of stress. In fact, this condition ensures that Coulomb's friction law is obeyed in any plane within a material element. The full Mohr-Coulomb yield condition consists of six yield functions when formulated in terms of principal stresses and six plastic potential functions (Plaxis 3D Foundation Manual, 2006).

The two plastic model parameters appearing in the yield functions are the well-known friction angle ϕ and the cohesion c. The condition *fi=0* for all yield functions together (where, *fi* is used to denote each individual yield function) represent a hexagonal cone principal stress space as shown in the Figure 2.16.

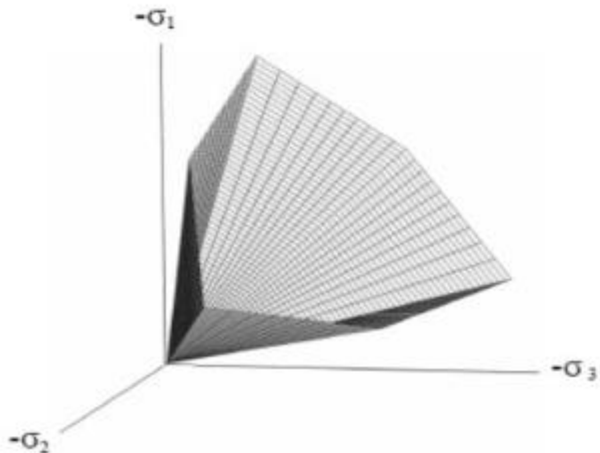


Figure 2.16: The Mohr-Coulomb yield surface in principal stress space (*c = 0*) (R.B.J. Brinkgreve and W. Broere, 2006)

The plastic potential functions contain a third plasticity parameter, the dilatancy angle ψ. This parameter is required to model positive plastic volumetric strain increments (dilatancy) as actually observed for dense soils. For stress states within the yield surface, the behavior is elastic and obeys Hooke's law isotropic linear elasticity, as discussed above (Plaxis 3D Foundation Manual, 2006).

# 3. Materials and Methods

## 3.1. General description of study area

### 3.1.1. Location

The study area is in Addis Ababa, Bole Bulbula. In this area, there are high-rise buildings.

### 3.1.2. Geology and Subsurface Condition

**Regional Geology**

Addis Ababa city is situated in the western margin of the Main Ethiopian Rift and represents a transition zone between the Ethiopian Plateau and the rift with poorly defined escarpment.

The geology of Addis Ababa area is represented by four volcanic units dominated in the lower part by basaltic lava flows (Addis Ababa basalt), followed by a pyroclastic sequence, mainly formed by ignimbrites (Addis Ababa Ignimbrite), followed by central composite volcanoes (Central Volcanoes unit), and finally small spatter cones and lava flows (Akaki unit).

Addis Ababa city is situated in the western margin of the Main Ethiopian Rift and represents a transition zone between the Ethiopian Plateau and the rift with poorly defined escarpment.

The geology of Addis Ababa area is represented by four volcanic units dominated in the lower part by basaltic lava flows (Addis Ababa basalt), followed by a pyroclastic sequence, mainly formed by ignimbrites (Addis Ababa Ignimbrite), followed by central composite volcanoes (Central Volcanoes unit), and finally small spatter cones and lava flows (Akaki unit).

Addis Ababa basalt extensively crops out along Akaki, Kebena, and Dukem rivers at the east to southeastern part of Addis Ababa, and represents the oldest unit of the area. It consists of essentially sub-horizontal lava flows with thickness ranging from few meters up to 20m. Maximum exposed thickness was found east of Addis Ababa, along the Kebena River. Addis Ababa basalt is predominantly constituted by alkaline and olivine basalts with three main textural attributes, that is, porphyritic, aphyric, and sub-aphyric.

Addis Ababa Ignimbrite is exposed close to Addis Ababa along the Akaki and Kebena rivers. It overlies the Addis Ababa basalt and locally covers the products of the composite central volcanoes of Wechecha and Furi. Different flow units constitute the sequence, consisting of pale-green to pale-yellow welded and crystal rich ignimbrites.

Central volcanoes unit includes the Yerer volcano and the product of the two composite volcanoes wechecha and Furi west and southeast of Addis Ababa, respectively. Wechecha and Furi volcanoes are two large edifices composed by predominant trachyte with minor pyroclastics. Yerer represents the largest volcanic edifice in the region, with a relief of 1000m from the plain and 14km wide along east-west direction. Products mainly consist of trachytes, even if pyroclastics are widespread mainly in the central part eastern sector. The highest part of Yerer volcano was affected by a more recent volcanic activity that produces spatter cones and associated basalt.

Akaki unit crops out east of Addis Ababa and consists of scoria and spatter cones with associated tabular lava flows and phreato- magmatic deposits. Alluvial deposits covering these units consists of regolith, reddish brown soils, talus, and alluvium with maximum thickness of about two meters. Geologic map of the project area is shown in figure below.

**Site Geology and Subsurface Condition**

The selected site and its surroundings are covered with made ground at the top underlain by silt-CLAY and sandy silty-CLAY developed from complete weathering of underlying vesicular BASALT. Sub-surface investigation done by Arcon design built for the construction 2B+G+13 mixed-use building in Addis Ababa Bole area has confirmed the presence of made ground, silty CLAY, sandy silty CLAY, and medium strong vesicular BASALT. The geological section showing lateral and vertical extent of these layers is shown in Appendix B.

**Ground water Observation**

Measurement of ground water level was made on the borehole. Drilling operation recorded that there were no ground water boreholes within depth of 60m (Arcon design-built Plc, 2017).

## 3.2. Methodologies

The study was conducted using the finite element software PLAXIS 3D. The software was used to simulate the lateral response of a single pile loaded horizontally in layered soil. The study considered varying the pile diameters and lengths, and loading eccentricity.

The model was generated in PLAXIS 3D using the column method. The column method is used to simulate pile-soil interaction by dividing the pile and soil into several columns. The mesh size was determined by conducting a sensitivity analysis to ensure accurate results.

The secondary soil data for the case of Addis Ababa Bole Bulbula area were modeled using Mohr-Coulomb material properties. The elastic modulus, Poisson's ratio, friction angle, and cohesion of the soil were used as input parameters. The pile was modeled using elastic material properties.

The model's accuracy was validated by comparing the numerical results with previously published experimental data. A good correlation between the numerical results and the experimental data was acceptable.

The results obtained from the numerical simulation of the lateral response of a single pile were discussed. The whole process was documented in the final report together with the important conclusions and recommendations.

## 3.3. Parameters used for the base model

To obtain a pile head stiffness that represents a wide range of practical problems for static laterally loaded pile, soil and pile properties are involved.

### 3.3.1. Soil parameters

The basic elements for analysis laterally loaded pile foundations are identifying parameters for base model, using in-situ test or correlations of parameters. Based on the investigations made by (Arcon design-built Plc, 2017) a representative value of SPT test data were chosen. The required soil parameter correlations were selected based on data quality, soil profile, consistency, and availability. The soil considered for this study were taken from Addis Ababa around Bole Bulbula area. Ground water level was not found in borehole depth, which is 60m from natural ground level. Therefore, the effect of water was not considered in this thesis. The engineering design parameters were extracted from SPT N values of representative borehole log sheet, which was conducted by (Arcon design-built Plc, 2017) and considered to represent the soil in study area. The representative borehole-log sheet and the cross-section are shown in the appendix A. The soil parameters obtained from the correlation of SPTN values were used as input parameters for PLAXIS 3D. These parameters are shown in table in 3.1.

Table 3.1: Soil Parameters for Base Model from SPT correlation.

| Depth (m) | Descriptions | E (MPa) | poison's ratio (v) | Unit weight (bulk) | c (MPa) | friction angle (ϕ) |
|---|---|---|---|---|---|---|
| 2.7 | Backfill silt-gravely ***SILT*** | 12 | 0.3 | 16 | 0.015 | 27 |
| 11.05 | Stiff to hard, light grey, high to ***low plastic clayey SILT(ML)*** sandy SILT/ weathered product of IGNIMBRITE | 15 | 0.3 | 16 | 0.012 | 28 |
| 12.6 | Hard, light brown, ***low plastic clayey SILT(ML)*** with trace sand | 13 | 0.3 | 17 | 0.065 | 32 |
| 25.45 | Extremely weak to medium strong, dark grey to very closely fractured, ***moderately weathered TRACHYBASALT*** | 1200 | 0.26 | 24 | 5 | 45 |
| 29.9 | Medium strong to very weak, dark grey, moderately weathered, closely to very closely ***fractured TRACHYBASALT*** | 1500 | 0.19 | 26 | 5 | 45 |
| 32.5 | Very weak to extremely weak, variegated color, moderately to highly weathered, very closely to very ***fractured TRACHYBASALTS*** | 400 | 0.27 | 20 | 0.03 | 42 |
| 60 | Medium strong to very weak, dark grey, moderately to very closely jointed ***vesicular TRACHYBASALT*** | 1000 | 0.26 | 22 | 5 | 42 |

## 3.4. Parameters of reinforced concrete circular pile used for the model

To understand the effect of pile properties on the lateral response of single piles, an effort is made to include a wide range of piles. The parameters described in the following sections are considered based on their use in practice.

Most of the time, reinforced concrete is used in the construction of pile foundations. Due to this reason, more emphasis is given to reinforced concrete piles. So, the material properties listed below are only for reinforced concrete. However, this does not indicate that the model is not calibrated for piles made of other materials.

**Pile Young's modulus ($\boldsymbol{Ep}$)**

According to EN 1992.1.-2004 (Part 1.1, Table 3.1), the modulus of elasticity varies depending on the compressive strength of concrete and is given by Equation (3.1)

$E_{cm} = 22\left(\frac{f_{cm}}{10}\right)^{0.3}$ ......................................................................................................*Equation 3.1*

Where, $f_{cm} = f_{ck} + 8MPa$ and $f_{ck}$ is the characteristics compressive strength, and $f_{cm}$ is in $(N/mm^2)$.

In most pile foundation construction projects, the value of $f_{ck}$ varies between 16 to 40 MPa (C 20 – C 50). The modulus of elasticity under consideration is selected as 30 GPa for $f_{ck} = 20MPa$ (C 25).

**Pile diameter and lengths**

The effect of length and diameter of the pile is included in the analysis with loading eccentricities.

Table 3.2: Pile parameters

| Parameter | Symbol | Pile-1 | Pile-2 | Pile-3 | Pile-4 | unit |
|---|---|---|---|---|---|---|
| Material | | Concrete | Concrete | Concrete | Concrete | |
| Modulus of elasticity | E | 30 | 30 | 30 | 30 | GPa |
| Poisson's ratio | $\nu$ | 0.15 | 0.15 | 0.15 | 0.15 | - |
| Unit weight | γ | 25 | 25 | 25 | 25 | $k/m^3$ |
| Length | L | 15 | 20 | 25 | 30 | m |

Table 3.3: Pile diameters and lengths

| Eccentricity (e/d) | | | |
|---|---|---|---|
| 0 | 2 | 4 | 6 |
| Embedded pile length L(m) | | Pile diameter D (m) | |
| 15 | | 0.5 | |
| | | 0.8 | |
| | | 1.1 | |
| | | 1.4 | |
| 20 | | 0.5 | |
| | | 0.8 | |
| | | 1.1 | |
| | | 1.4 | |
| 25 | | 0.5 | |
| | | 0.8 | |
| | | 1.1 | |
| | | 1.4 | |
| 30 | | 0.5 | |
| | | 0.8 | |
| | | 1.1 | |
| | | 1.4 | |

# 4. Numerical Modeling

## 4.1. Introduction

In this study, Plaxis 3D was used in geometry modelling to investigate the response of laterally loaded piles in soils of the study area. Verification of the study with full-scale lateral load tests result from the literature was used to control the accuracy of the numerical model results. After verification of finite element analysis solution, a parametric study has been conducted (chapter-5). Variations in the factors such as the embedment depth of the pile, pile diameter, and loading eccentricity. In this chapter, properties and main functions of the 3D finite element methodologies presented briefly for better understanding of the model designs.

## 4.2. Overview of PLAXIS 3D FOUNDATION

Plaxis 3D Foundation is a three-dimensional finite element program used to perform deformation and stability analysis for various types of geotechnical structures such as foundations, anchors, and sheet piles. The program uses a convenient graphical user interface that enables users to generate a geometry model and a finite element mesh quickly and easily. Plaxis 3D Foundation is an implicit element solver relating forces and displacements by demanding equilibrium in every point in the model.

The generation of a three-dimensional finite element model is based on the model geometry such as volumes, surfaces, lines, and points. To create the soil stratigraphy different boreholes can be defined. Boreholes are locations in the drawn area at which the information on the position of soil layers and the water table is given. The program will interpolate the soil layer position between each borehole.

The sign convention used by Plaxis 3D Foundation was based on the Cartesian coordinate system as shown in Figure 4.1.

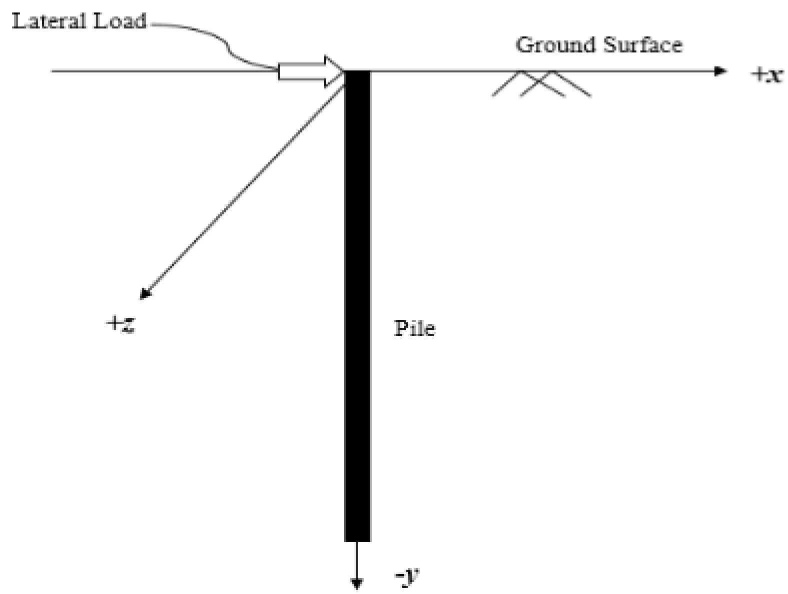


Figure 4.1: General three-dimensional coordinate system and sign convention for the model

The creation of the model consists of two parts, generation of the model and calculation phase. The model geometry is a composition of boreholes and work planes. Only one borehole is created in the numerical modelling, as no information on the soil stratigraphy at the site is available, i.e. the soil layers are assumed horizontal and homogenous. The work planes are used in order to define loads and structures at different vertical levels. Soil and material properties can be added using material library in Plaxis 3D Foundation, where standards values of the material properties of construction materials can be found. For these numerical approaches, the soil material assignment depending on the soil properties obtained from correlation of different parameters using SPT-N values, UCS and triaxial tests obtained from the geotechnical laboratory and field tests.

Plaxis 3D Foundation consists of two parts, which are input and output program. Input program is used for the definition of the model and assignment of analysis properties. At the beginning of the input program, project properties are asked from the user. Model boundaries in two horizontal directions (*x* and *z*) and unit system used in analyses are defined in this part. Input program includes five main components that are soil, structures, mesh, water levels and staged construction. In soil mode, soil stratigraphy is assigned to the model by creating boreholes. In addition, ground water level of a specific point is defined also with boreholes. Multiple boreholes can be defined in any number at any point. Work planes are horizontal planes with different y-coordinates that show the top view of the model geometry. They were used to draw, activate, and deactivate the structural elements and loads. Each work-plane holds the same geometry lines but vertical distance between them may vary. Within work-planes, points, line sand clusters were used to describe a 2D geometry model.

Plaxis 3D Foundation interpolates layer thicknesses and ground water levels that were assigned in every borehole. Desired non-uniform three-dimensional soil profiles and water level can be obtained with this way. In structures mode, all kinds of geometric entities, structural elements and their configurations were assigned. In addition, boundary conditions; predefined displacement or loading of a point, line or a surface can be defined in this part. Both soil and structure modes include material sets option that was used for the definition of material properties of soil and structural elements. In mesh mode, geometry was divided into mesh elements with desired amount of fineness.

There are five standard mesh element distributions in Plaxis 3D Foundation. These are very coarse, coarse, medium, fine, and very fine mesh generations. In addition, desired amount of local fineness of a specific volume or geometric entity can be achieved with fineness factor option. In water levels mode, water levels outside of the model can be defined for the simulation of external water pressures. Additionally, it can be used as phreatic level for partially saturated soils. After finalization of all geometric entries, calculation stages were arranged in staged construction mode according to the purpose of the analysis. All geometric elements can be activated or deactivated for every stage. Besides, analysis properties of each stage such as calculation type, maximum number of iteration and error tolerance can be defined separately. After setup of all stages, analysis can be conducted.

Plaxis 3D Foundation provides extensive ways for the documentation of the analysis results. Output program was presented all numerical analysis results in variety of forms including curves, diagrams, and tables. It mainly consists of the results of deformations and stresses. In addition, force results are presented for structural elements. This chapter is devoted to introduce the details of constitutive models, material properties, and finite element modelling used in the performed parametric study.

## 4.3. Generation of the Model

### 4.3.1. Model Geometry

In this part of the research, geometry modelling was conducted on a single pile in layered soil by using Plaxis 3D Foundation FEM package. The pile was modeled using a volume pile model available in Plaxis 3D Foundation. The model geometry depends on both the diameter of pile and its length. The soil is layered and the cross section of the soil block was pre-defined in the model tab on the project properties window. Based on the pile geometry, the limits of the soil contour were defined as the $x_{min}, x_{max}$ $and$ $z_{min}, z_{max}$ . The depth (y-axis) was applied using the "create borehole" button, in this function groundwater table, level can also be selected. The top boundary of the soil layer is at y = 0, and the bottom boundary of the soil layer is a function of pile diameter and its length. Once the soil block was drawn, the soil properties can be assigned to it.

According to (Karthigeyan et al., 2007) for static lateral load condition, the soil mass dimension depends on the pile diameter and length. The width of soil mass was taken as 40D, in which, D is the pile diameter or pile width. The soil mass effect on the pile response is diminishing for the width more than 40D. The height of soil mass was taken as L+20D, in which, L is the length of pile as shown in Figure 4.2.

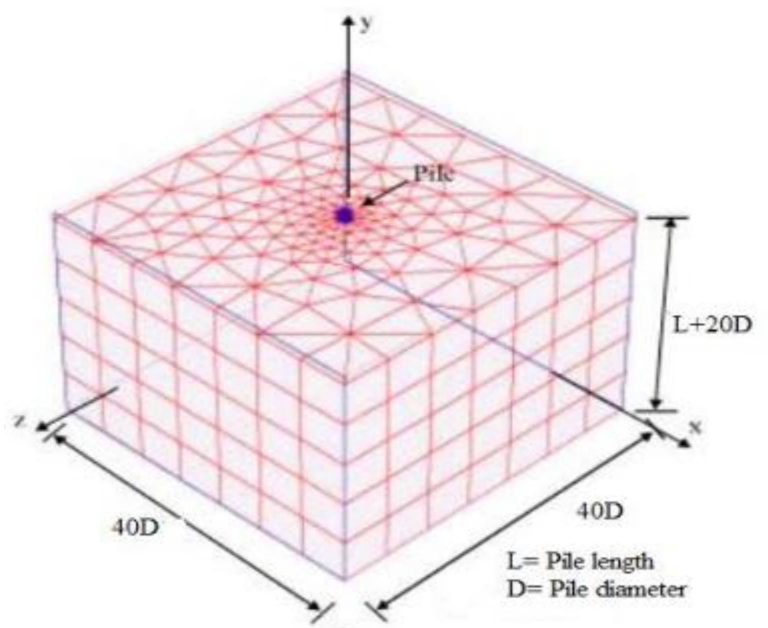


Figure 4.2:3D finite element mesh for soil mass and location of pile.

Table 4.1: 3D FEM model dimensions (design of experiments)

| Embedded pile length L(m) | Pile diameter D (m) | Width of soil mass along X (m) | Length of soil mass along Z(m) | Height of soil mass along Y (m) |
|---|---|---|---|---|
| 15 | 0.5 | 20 | 20 | 25 |
| | 0.8 | 32 | 32 | 31 |
| | 1.1 | 44 | 44 | 37 |
| | 1.4 | 56 | 56 | 43 |
| 20 | 0.5 | 20 | 20 | 30 |
| | 0.8 | 32 | 32 | 36 |
| | 1.1 | 44 | 44 | 42 |
| | 1.4 | 56 | 56 | 48 |
| 25 | 0.5 | 20 | 20 | 35 |
| | 0.8 | 32 | 32 | 41 |
| | 1.1 | 44 | 44 | 47 |
| | 1.4 | 56 | 56 | 53 |
| 30 | 0.5 | 20 | 20 | 40 |
| | 0.8 | 32 | 32 | 46 |
| | 1.1 | 44 | 44 | 52 |
| | 1.4 | 56 | 56 | 58 |

### 4.3.2. Model Properties

Finite element analysis software Plaxis 3D Foundation was used for the investigation of the lateral response of laterally loaded pile. In order to carry out a parametric study, other properties should be kept constant while the effect of the change in a certain property was being investigated. Therefore, the interpretation of parametric study results can be more complex, since the effect of several factors will interfere with each other. In addition, actual laterally loaded pile model with all external boundaries will require much more 3D mesh elements, which cause longer calculation times.

Volume pile option in Plaxis 3D was used to model the vertical pile and its properties in all analyses. This option was given the opportunity of modelling piles as structural members with a definite rigidity and mechanical properties.

Before systematically investigating the factors affecting the pile-soil interaction behavior, the boundary size, surface fixity conditions, and mesh generation effects were studied, as it is necessary in order to establish correct geometry and model of the problem.

### 4.3.3. Model Boundary Fixities

The boundaries of the soil in the model must be constrained in the vertical and lateral directions where the displacement of the soil due to the lateral load is negligible. In order to minimize the boundary effects in the model many authors suggested different locations of these boundaries. The horizontal length extent of 40D (40 times of the pile diameter) and vertical depth extent of L+20D (length of a pile plus 20 times diameter of a pile) is enough after which no appreciable stress and strain variation effect was observed.

Therefore, boundaries of the model were placed at enough distances from the pile so that the influence of the boundaries on the deformations of the pile is minimized. Three separate boundary conditions were imposed onto the model. Nodes on both lateral boundaries of the model were fixed against horizontal movement($u_x = u_y = u_z = 0$), yet free to move in the horizontal direction. Meanwhile, nodes on the bottom boundary of the model were fixed against all directions($u_x = u_y = u_z = 0$), whereas the top boundary was free to move in all directions.

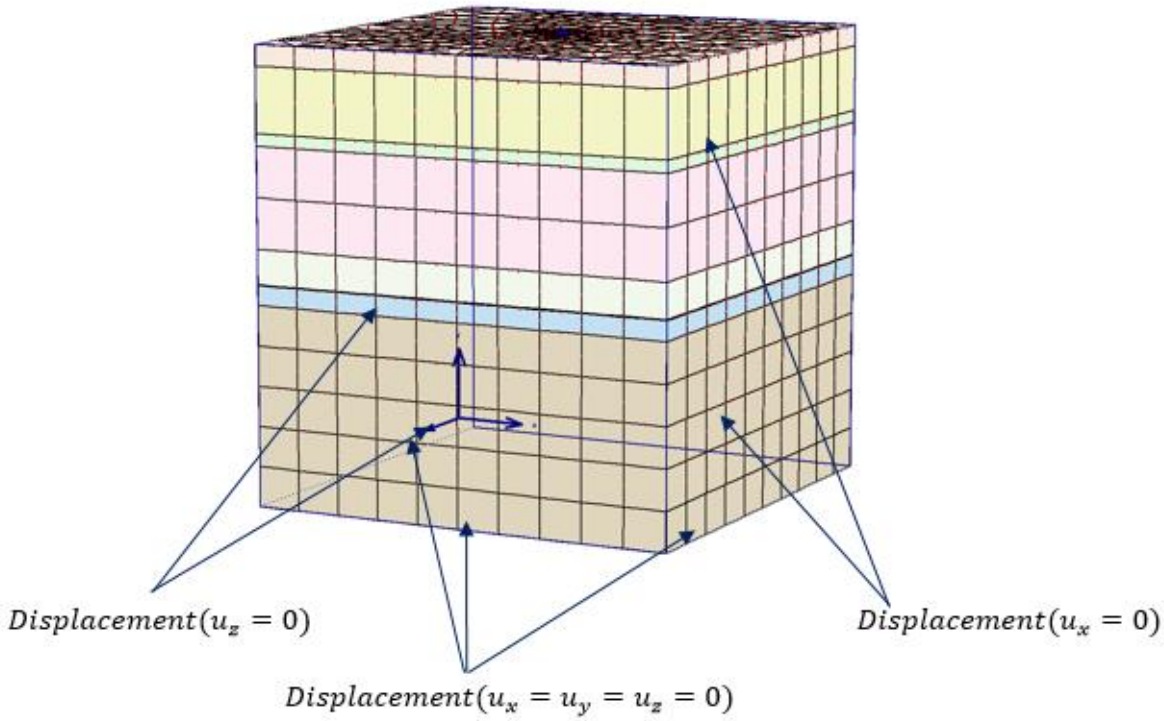


Figure 4.3: Boundary conditions

It is desirable to select the size/geometry of the model large enough so that boundaries are far away from the area where we are making calculations, and that stress-strain distributions in the soil are not affected from the geometrical constraints near the boundaries. However, long calculation times in three-dimensional analyses make this procedure inefficient.

Therefore, the size/geometry of the model and distance to the boundaries were studied to determine the optimum dimensions enough for an accurate model. The deflections in the soil were investigated as a result of pile resistance are not affected or interrupted because of the model boundaries.

### 4.3.4. Mesh Generation

In order to perform the finite element calculations, the geometry must be divided into elements. A composition of finite elements is called a finite element mesh. The basic soil elements of a 3D finite element mesh were represented by the 15-node wedge elements. These elements were generated from the 6-node triangular elements. The 15-node wedge element was composed of 6-node triangles in horizontal direction and 8-node quadrilaterals in vertical direction.

The model was meshed using the automatic mesh generation tool in Plaxis 3D Foundation. The element was provided a second-order interpolation of displacements as shown in Figure 4.4. Plaxis 3D Foundation uses three local coordinates ($\xi$, $\eta$, $\zeta$), the shape functions have the property that the function value is equal to unity at node *i*, and zero at the other nodes. This type of element has three translational degrees of freedom in each node and is generated from 6-nodes triangular wedge elements, suitable for a two-dimensional mesh.

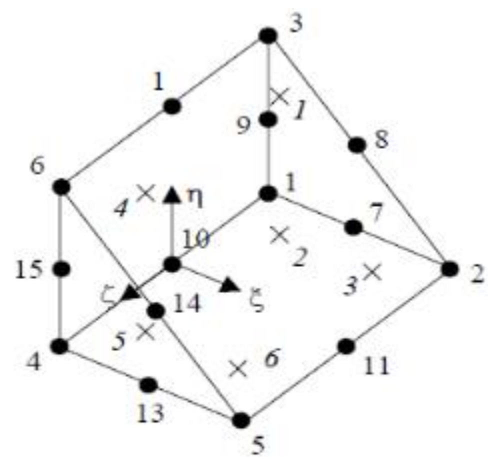


Figure 4.4: Local numbering and positioning of nodes (•) and integration points (x) of a 10-node wedge element in Plaxis 3D Foundation (Plaxis 3D Foundation Manual, 2006)

Typical 2D and 3D meshes used in this study were presented in Figure 4.5 and Figure 4.6, respectively. The mesh element size can be adjusted by using a general mesh size varying from very coarse to very fine and by using line, cluster, and point refinements. Very fines mesh should be avoided in order to reduce the number of elements, thus to reduce the memory consumption and calculation time. The program does not allow entering a new structural element or a new soil cluster after the mesh was generated. If a new element or cluster was added to the geometry model, the mesh generation should be repeated with the new input.

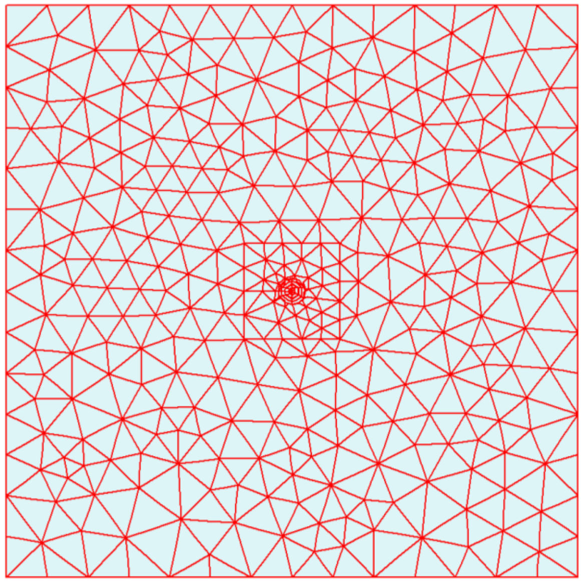

Figure 4.5: Mesh generation of the cross section of a typical 2D FE model

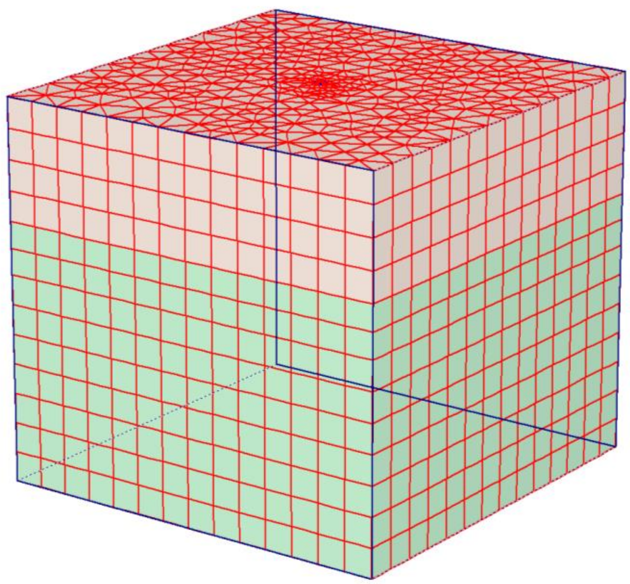

Figure 4.6: Mesh generation of a typical 3D FE model

3D finite element mesh was composed of elements, nodes, and stress points. While generating the mesh, the geometry was divided into 15-node wedge elements. As mentioned before, these elements were composed of the 6-node triangles in x-z direction, as generated by 2D mesh generation. Moreover, 8-node quadrilateral faces were generated in y-direction

### 4.3.5. Sensitivity Analysis

As mentioned above, in the finite element calculations, the model has divided into elements, which compose the "finite element mesh". The finite element mesh size will possibly influence the results. To investigate the influence of number of elements or mesh coarseness on the behavior of laterally loaded pile foundation, five different finite element meshes were performed. These were done by varying their number and sizes keeping material properties and all other parameters constant. For this purpose, a horizontal load of 180kN was applied at the pile head. The generated number of elements and the head deflection of a pile is given in Table 4.2.

Table 4.2: Influence of mesh size on head deflection

| Model | Mesh Coarseness | Number of elements | Head deflection (mm) |
|---|---|---|---|
| 1 | Very Coarse | 570 | 18.97 |
| 2 | Coarse | 952 | 18.44 |
| 3 | Medium | 3420 | 20.27 |
| 4 | Fine | 8632 | 20.1 |
| 5 | Very Fine | 20596 | 19.81 |

Table 4.2 shows the influence of mesh density on the head deflection of the pile. As shown from the figure head deflection is increases with increases number of elements until the number of elements reach 3420, after that an increasing in number of elements has no significant effect on the head deflection of pile. It can be said that mesh is converged with 3420 elements because there is no significant change in deflection when the number of elements increased to 20596. Therefore model 3 (medium mesh) was used to investigate the general lateral response of the laterally loaded pile foundation.

### 4.3.6. Calculation Process

At this phase the construction of the model and loads applied were staged. The first phase is the initial phase, where the initial stresses in the soil are computed using the $K_o$- procedure. In this procedure, the initial vertical stresses were computed using submerged soil unit weight. Then, related horizontal stresses were computed using the coefficient of lateral earth pressure at rest $K_o \cong \sin\varphi$, assuming normally consolidated soil.

Following the initial phase, a second phase called the installation phase was initiated. In the installation phase the pile foundation was constructed, the pile and interface surfaces were activated. Afterwards, the lateral load was applied at the ground surface of the top head of the pile. The load was applied using same intervals of load, and each interval corresponds to a different phase. The calculation phase was staged in this order, because the displacements were reset to zero after the initial stresses have been calculated and the foundation has been installed. This was done to calculate the lateral deflections, bending moments and shear forces created by the applied loads.

The staging is summarized below:

1. Calculation of initial stresses using the *Ko*- procedure.
2. The interface is activated and the pile was installed.
3. The horizontal load was applied in different phases corresponding to increments of load.

A calculation process in Plaxis 3D Foundation was divided into calculation phases. In each calculation phase, numbers of calculation steps are needed since the non-linear behavior of the soil requires loadings in small proportions (load steps) as shown in Figure 4.7.

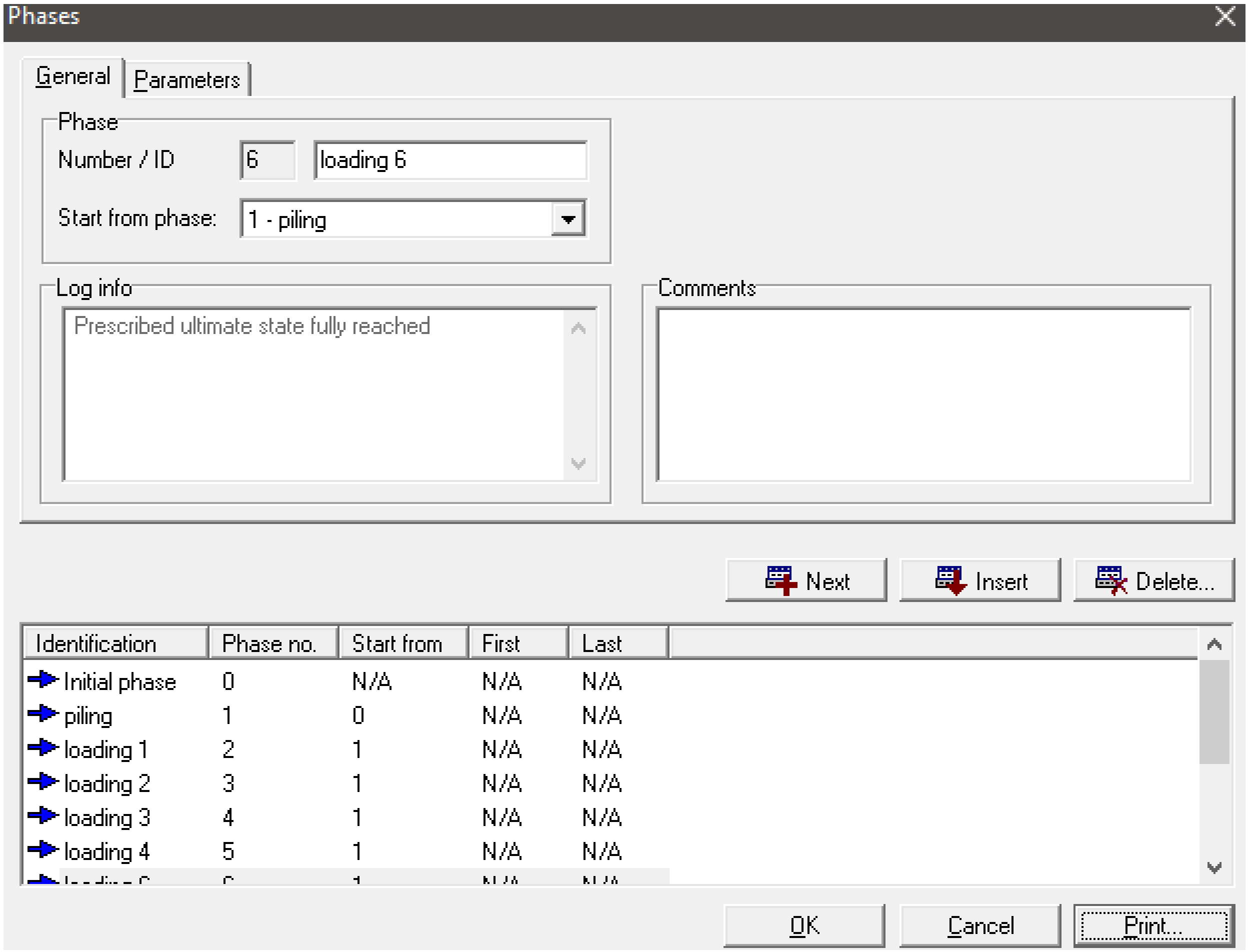


Figure 4.7: Calculation phases in Plaxis 3D Foundation

### 4.3.7. Interface Element

In order to achieve a good relationship between the pile structure and the soil volume, an interface was created. Interfaces were joint elements to be added to the surfaces to allow for a proper modelling of soil-structure interaction. Interfaces were used to simulate the contact between a plate (from the pile structure surfaces) and the surrounding soil. An interface can be created next to the plate or geogrid elements or between two soil volumes. In the model, the interface was created next to the pile plates. The thickness of the interface was zero, which means that the pair of nodes were located with the same coordinates. The interface consists of 16 nodes quadrilateral shaped elements. Interface elements are numerically integrated using three Gauss integration points. Figure 4.8 shows the position of the nodes and integration points.

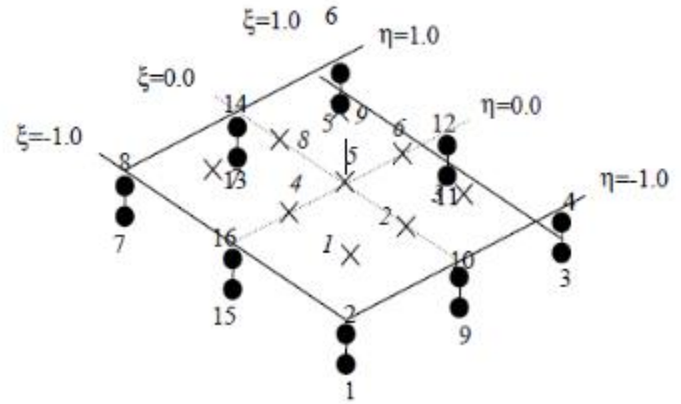


Figure 4.8: Local numbering and positioning of nodes (Ɛ) and integration points (x) of a 16-node interface element (Plaxis 3D Foundation Manual, 2006)

The interface elements have pairs of nodes instead of single nodes. The distance between the two nodes of a node pair is zero. The aim of these interface nodes is to allow for differential displacements between the node pairs slipping and gapping.

The interface stiffness and strength can be defined depending on the kind of analysis, and it is controlled by the parameter R*inter*. A rigid interface, perfectly rough soil-structure, is used when the interface should not have a reduced strength with respect to the strength of the surrounding soil. The strength of these interfaces was assigned as rigid (which corresponds to R*inter* = 1.0). It behaves as an element with the same material properties as the adjacent soil element. In thin layer element method, the contact between structure and soil was described as perfectly rough. The material behaviour in the contact area (the thin element) was simulated by the material behavior of the soil (Table 3.1, Table 3.2, and Table 3.3).

The following rules are applied to calculate the interface properties from the soil properties in the related data set and value of *Rinter*.

$c_{inter} = c_{soil}$ ……………………………………………………………………………*Equation 4.1*

$tan\phi_{inter} = tan\phi_{soil}$ ……………………………………………………………………*Equation 4.2*

Where: $c_{inter}$ –Cohesion of the interface

$c_{soil}$ -Cohesion of the soil

$tan\phi_{inter}$ –Interface friction angle

$tan\phi_{soil}$ –Soil friction angle

## 4.4. Validation of Numerical Model

The finite element approach was used in this study to investigate the lateral response of pile when subjected to lateral loads. This section used to assess the accuracy of the finite element approach in analyzing laterally loaded piles and to verify certain details of the finite element such as pile displacement. Verification example was worked out to compare the result obtained by finite element analysis to those obtained from experimental study. The comparative case includes full-scale lateral load tests reported by (F.Ismael, 1998). The results of laboratory and field tests are used to identify the soil profiles and soil properties that are well instrumented.

Table 4.3: Geotechnical properties of the soil layer

| Parameters | Name | Medium dense cemented silty sand layer | Medium dense to very dense silty sand | Pile | Unit |
|---|---|---|---|---|---|
| Unsaturated Soil Weight | $\gamma_{unsat}$ | 18 | 19 | 25 | $kNm^{-3}$ |
| Saturated soil weight | $\gamma_{sat}$ | 18 | 19 | - | $kNm^{-3}$ |
| Young's Modulus | E | 13000 | 13000 | 2.00E+09 | kPa |
| Poisson's Ratio | $\nu$ | 0.3 | 0.3 | 0.15 | - |
| Cohesion | c | 20 | 1 | - | kPa |
| Friction Angle | $\phi$ | 35 | 45 | - | ° |

The case study deals with lateral load in which the deflection response of bored piles in cemented sand was examined by field test on a single pile under lateral load (F.Ismael, 1998). All piles were 0.3m in diameter and had a length of 3 or 5m. The site of this load test was in Kuwait. The surface soil to a depth of 3.5m was characterized by having both component of shear strength, both effective parameters. The soil profile consists of a medium dense cemented silty sand layer to a depth of 3m. This is underlain by a medium dense to very dense silty sand with cemented lumps to the bottom of the borehole. The same load sequence as pile tests was applied to the pile after completing the whole geotechnical model for lateral pile tests. The properties of soil in the both cases are listed in Table 4.3.

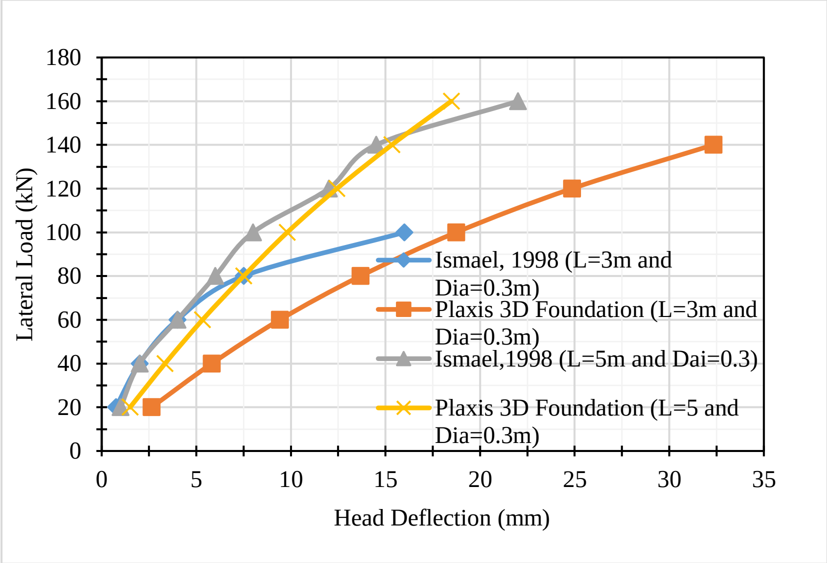


Figure 4.9: Comparison of finite element result with field test data from (F.Ismael, 1998).

The comparison between the finite element result and layered sand field test data is shown in Figure 4.9. The pile with a length of 5m is highly resistance to the lateral load from the second pile length value. Comparable data were obtained between the experimental results of the three piles and the present simulation model. The results obtained from the numerical simulation for a pile of 5m is relatively closed with the result obtained from the field test.

# 5. ANALYSIS AND PARAMETRIC STUDIES

## 5.1. Introduction

In this chapter, a parametric study was conducted on a laterally loaded pile embedded in layered soil conditions using Plaxis 3D Foundation. One of the purposes for this study was to investigate lateral response of laterally loaded pile by varying, length of the piles, pile diameter, and loading eccentricity under static lateral loading. To carry out this study, other properties should be kept constant while the effect of the change in a certain property is being investigated.

## 5.2. Results and Discussion

In order to evaluate the effect of some parameters due to laterally loaded pile on the deformation analysis, a parameter analysis was performed. To carry out this study, other properties should be kept constant while the effect of the change in a certain property is being investigated. The analysis result of some important parameters; pile length, pile diameter and loading eccentricity will be discussed.

### 5.2.1. Effect of Pile Diameter on Head Deflection

The lateral response of piles due to the loads applied at the ground surface on the piles head are drawn in Figures 5.1 to 5.4 for different embedded length and diameter of pile. These graphs show the change of lateral load and corresponding lateral deflection at the pile head in *x* direction. In Plaxis 3D Foundation the pile was modeled with diameter of pile 0.5, 0.8, 1.1 and 1.4m, and length of 15, 20, 25 and 30m for the same lateral loads of 250, 500 and 750kN.

In this section, the load displacement curves of different pile diameter and length will be used to assess the lateral response of horizontally loaded piles.

Figures 5.1 to 5.4 show lateral load and corresponding lateral head deflection at the pile head in *x* direction (*p-y* curves) at the end of FEM analysis. As it is observed in the *p-y* graph as the diameter of the pile increase there is a decrease in head deflection and vice versa for same constant loads. This was due to increase in surface area. In addition, the pile stiffness, EI, increase with increase in moment of inertia I, which depends on the diameter of the pile.

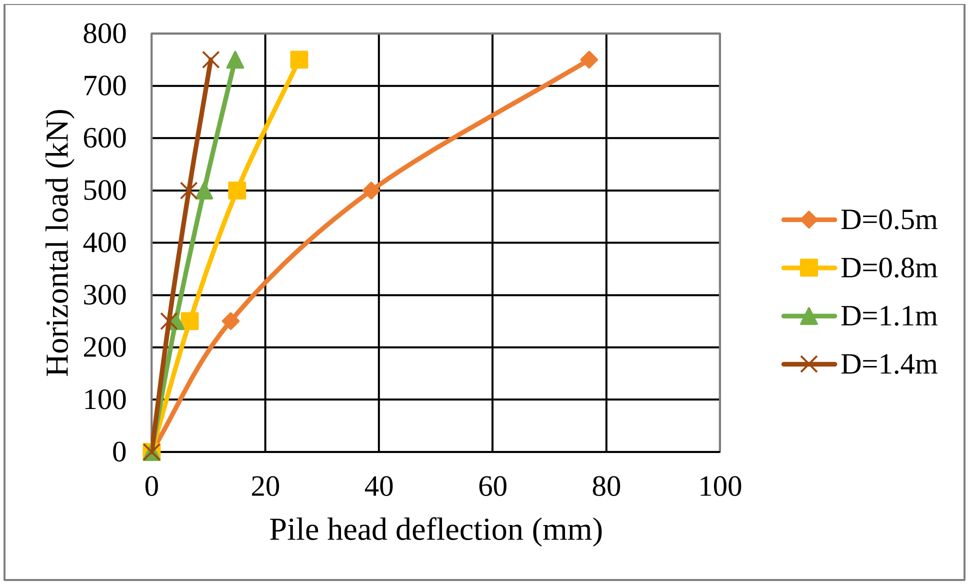


Figure 5.1: Lateral load versus head deflection of 15m pile length

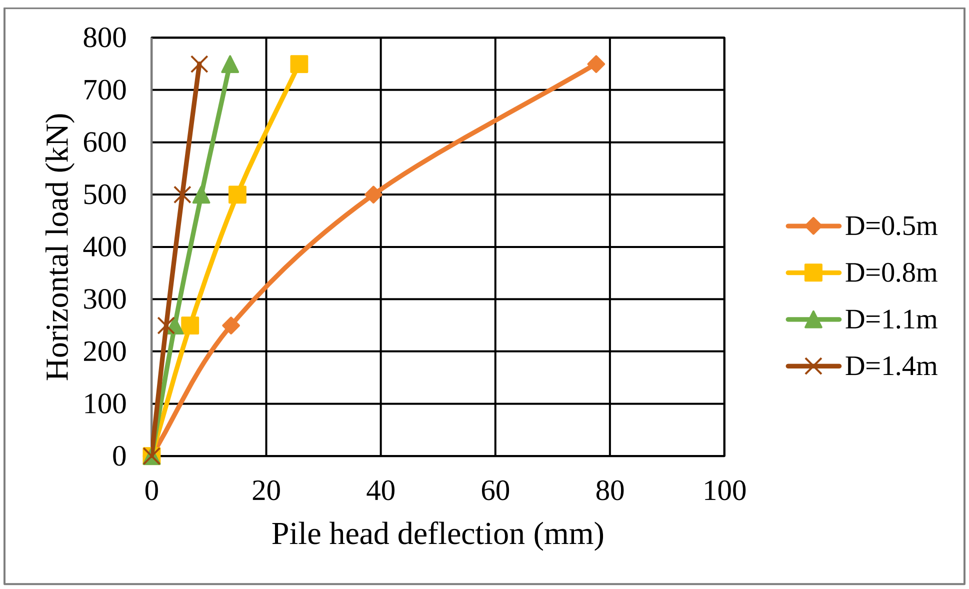


Figure 5.2: Lateral load versus head deflection of 20m pile length

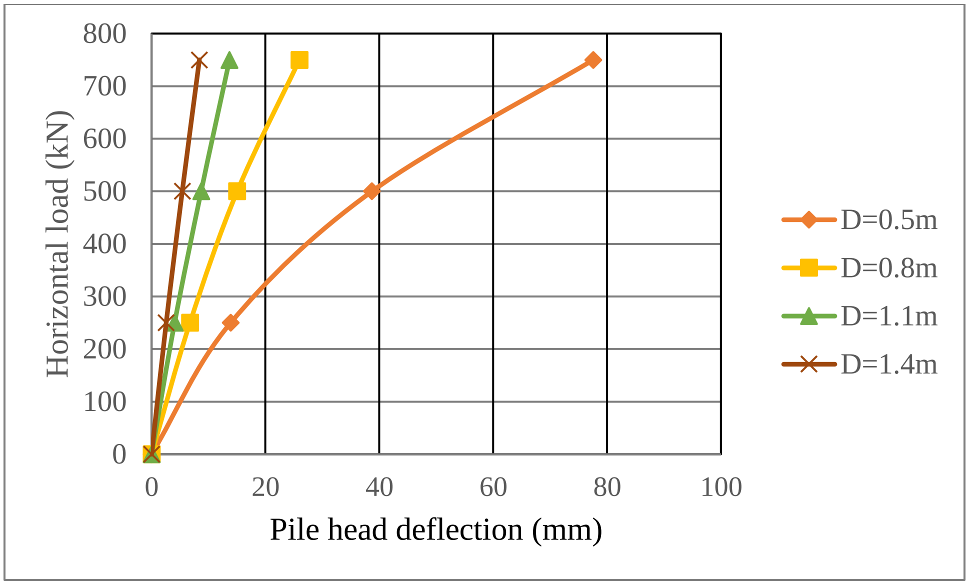


Figure 5.3: Lateral load versus head deflection of 25m pile length

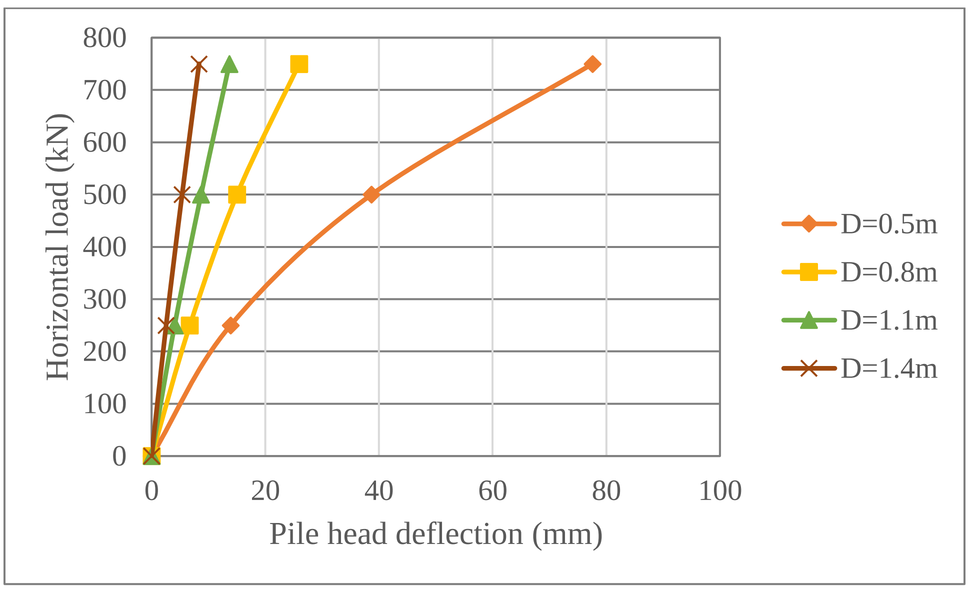


Figure 5.4: Lateral load versus head deflection of 30m pile length.

### 5.2.2. Effect of Length of the Pile on Head Deflection

The parametric study was carried out by varying the length of the pile and the deformation is obtained from Plaxis output. This parameter was varied for different pile length of 15, 20, 25, and 30m in the study. Figure 5.1, Figure 5.2, and Figure 5.3 shows that the results obtained from Plaxis 3D Foundation analysis. The pile head deflection and lateral load are obtained. It was observed that the length of the pile increased without increase in head deflection because the embedded length of the pile is greater than its critical length. All piles in this study were considered as flexible piles because they have length greater than its critical length Lc.

### 5.2.3. Effects of Loading Eccentricity, *e* on Head Deflection

The height of the pile above the ground is an excellent determinant on the moments above the ground level. The moment equilibrium equation is the product of the lateral force and the eccentricity. When the bending moments tend to increase then the ultimate load that the pile element can withstand reduces considerably. This reduction is due to the rotational effect produced by the lateral pressure above the ground level.

In this study, the loading eccentricity effect is evaluated at 0m, 1m, 2m and 3m for pile diameter of 0.5m and length of 15, 20, and 25 and 30m and same corresponding lateral loads.

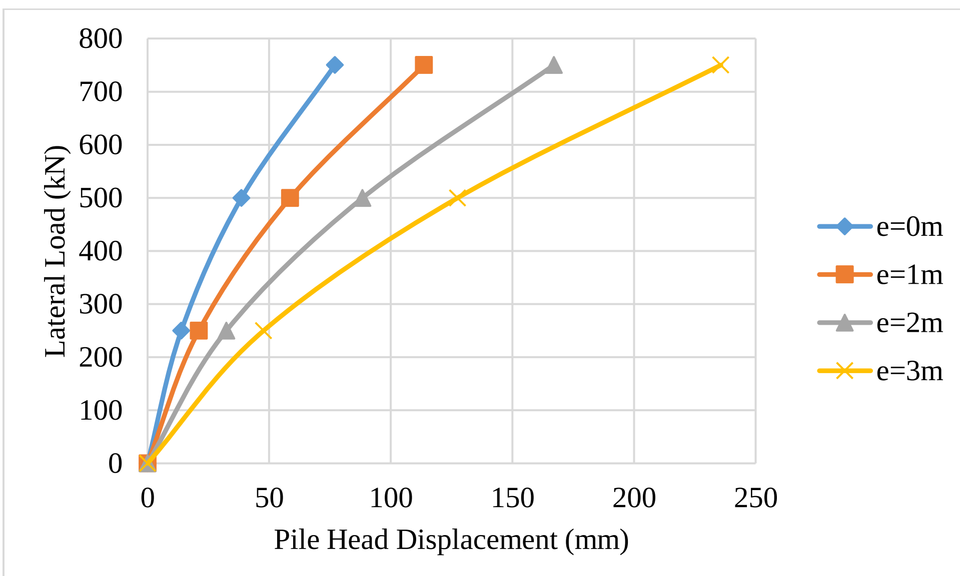


Figure 5.5: Lateral load versus head deflection of 15m pile length.

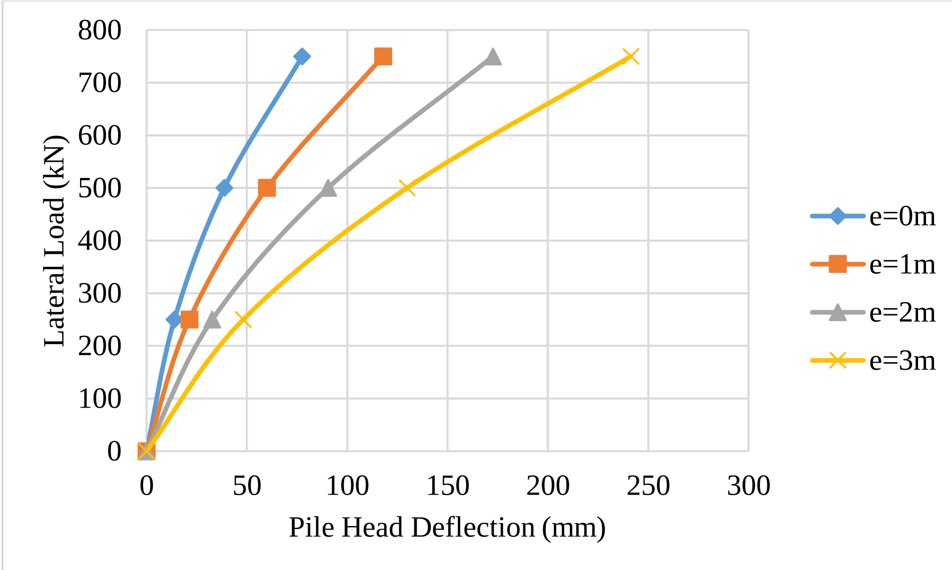


Figure 5.6: Lateral load versus head deflection of 20m pile length.

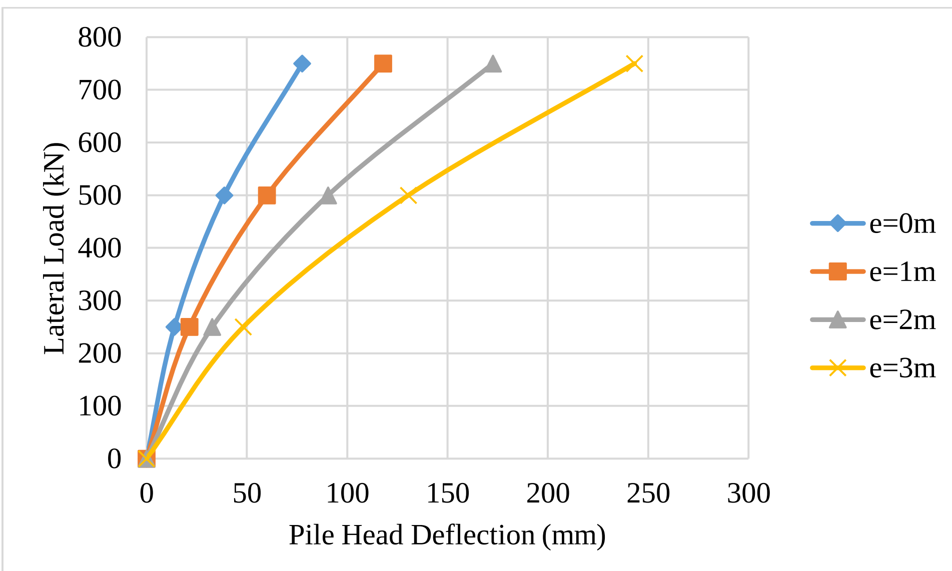


Figure 5.7: Lateral load versus head deflection of 25m pile length.

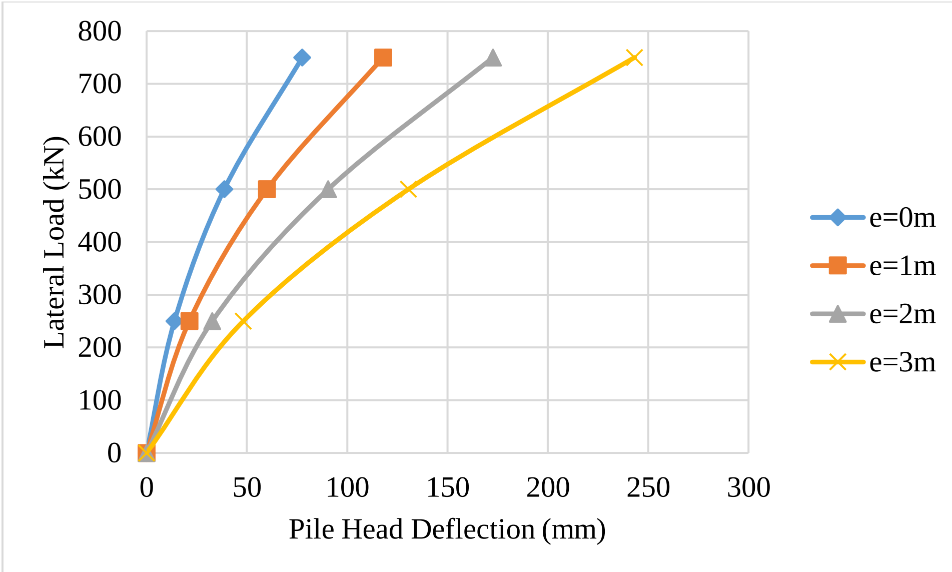


Figure 5.8: Lateral load versus head deflection of 30m pile length.

Figures 5.5-5.8 show the load displacement curve. Based on the results,

Increasing the load eccentricity from 0 to 1m, 1to 2m and 2 to 3m increases the pile head deflection by 34, 32 and 29% for the highest load respectively. Moreover, when load eccentricity increases from 0 to 3m the pile head deflection increases by 68%. This shows that the point of the load applied to a pile is a strong determinant of the ultimate strength concerning bearing capacity.

## 5.3. Ultimate Lateral Load Capacity from Numerical Results

The ultimate lateral resistance and working load deflections of single piles depends on the dimensions, strength, and flexibility of the individual pile, and on the deformation characteristics of the soil surrounding the loaded pile. The ultimate lateral resistance of a laterally loaded pile will be governed by the ultimate lateral resistance either of the surrounding soil or by the yield or ultimate moment resistance of the pile section.

The failure criterion considered in this analysis is the yield of the maximum ultimate lateral displacement at pile head, where the lateral load capacity of pile is reached when the ultimate lateral displacement yields at head of pile. The ultimate lateral displacement at pile head depends on some factors such as pile type, soil type, and type of structure carried by the pile, but it mainly depends on pile diameter.

The ultimate lateral load capacity of a pile referred in this thesis is taken as the loads corresponding to the lateral deflection at the pile head equal to around 10% of the diameter of the pile. In real design, the pile capacity may be even limited to deflection requirements, in another word, service limit conditions.

In all the cases studied, the load required to displace the pile head a horizontal distance equal to 10% of the pile diameter is assumed as the ultimate lateral load capacity of the pile. These ultimate loads are given in Table B-1, Appendix B.

The effects of diameter and length with different L/D ratio of a pile on its ultimate lateral load capacity is shown in Figures 5.9 to 5.12 obtained from 3D finite element method analyses.

### 5.3.1. Effect of Diameter of the Pile on Lateral Load Capacity

To study the effect of diameter on lateral load capacity of a pile having length 15, 20, 25, and 30m length with different diameters, 0.5, 0.8, 1.1, and 1.4m were considered. The results are given in Figure 5.9 to 5.12 which indicates that lateral load capacity increases with increasing diameter of the pile. This was due to the increase in surface area. In addition, the pile stiffness, EI, increases with increase in moment of inertia I, which depends on the diameter of pile.

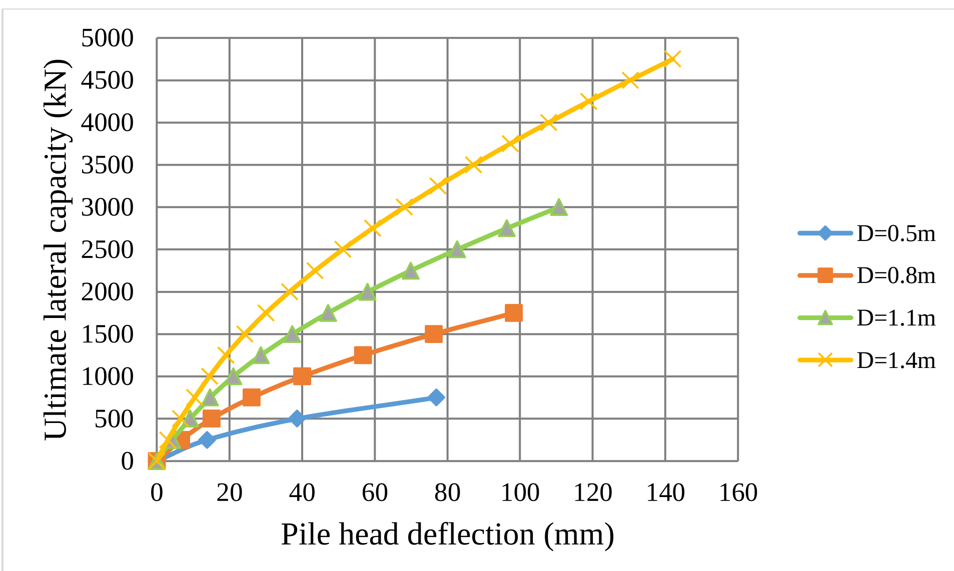


Figure 5.9: The effect of change in diameter on lateral capacity pile with length 15m.

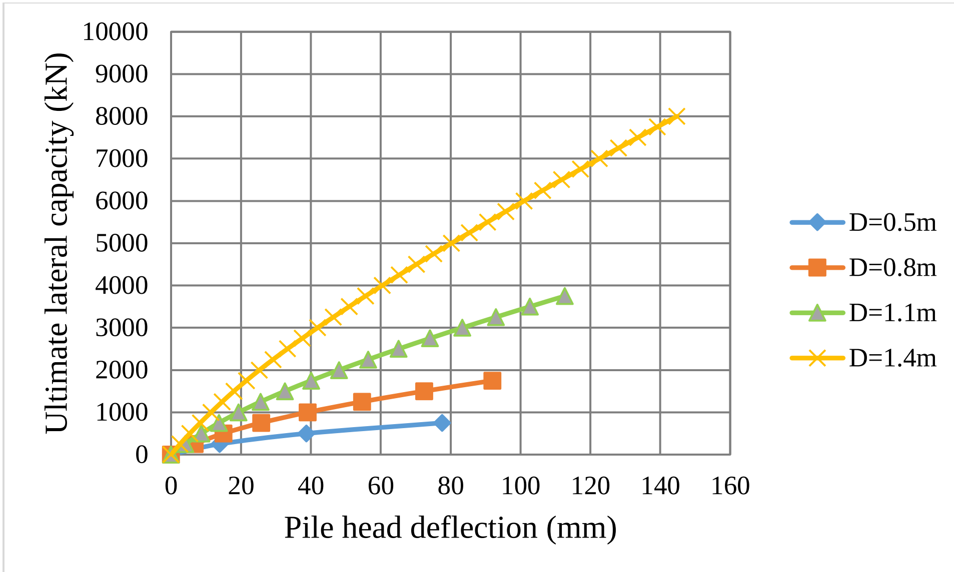


Figure 5.10: The effect of change in diameter on lateral capacity pile with length 20m.

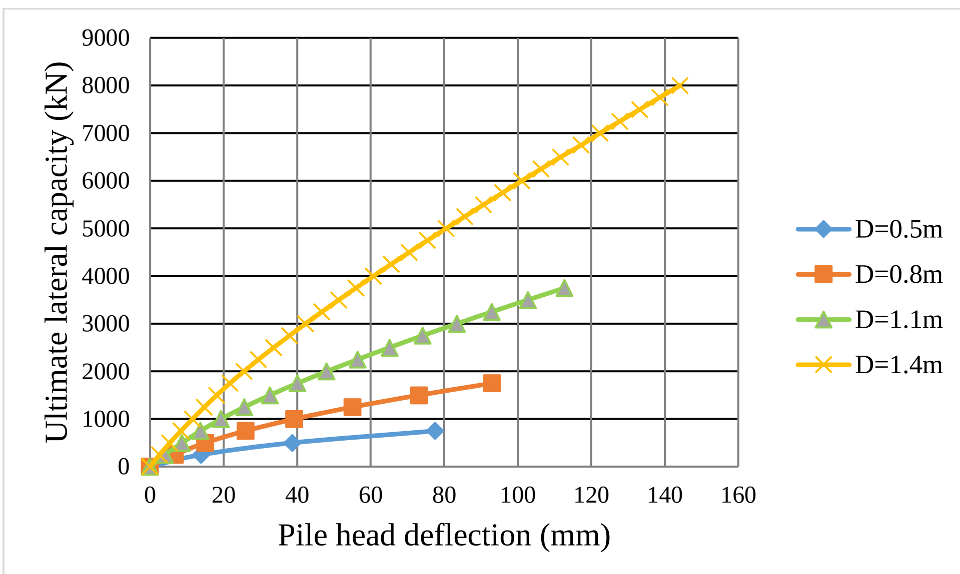


Figure 5.11: The effect of change in diameter on lateral capacity pile with length 25m.

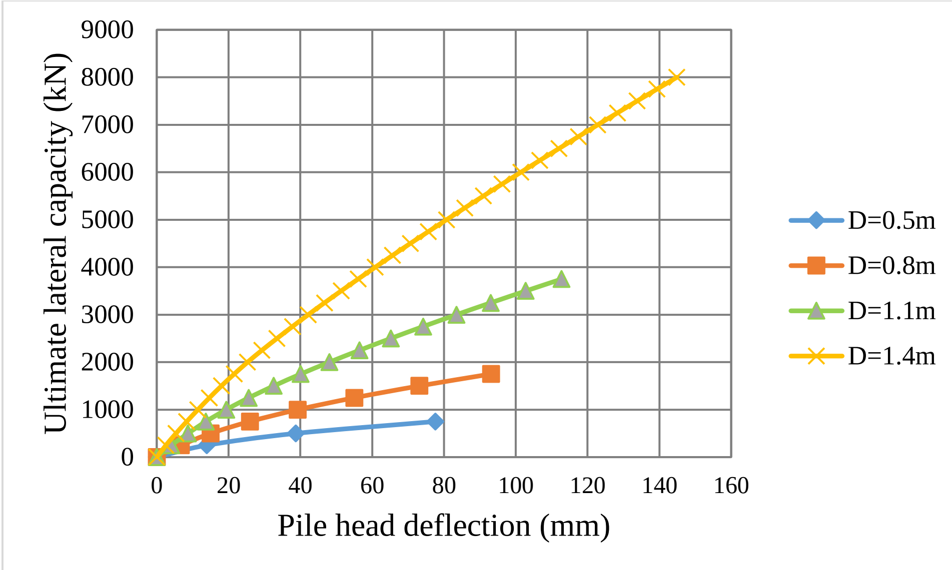


Figure 5.12: The effect of change in diameter on lateral capacity pile with length 30m.

The ultimate lateral capacity is increased by 62, 48 and 37% when the diameter changes from 0.5 to 0.8m, 0.8 to 1.1m and 1.1 to 1.4m respectively for pile length of 15m. And increased by 64, 57 and 53% for same changes of diameter with 15m pile length for 20, 25 and 30m pile lengths. This implies that with constant pile length and decreasing pile diameter, the ultimate lateral resistance of the pile decreased and he reverse is true. This shows that pile diameter has significant effect on lateral capacity of the pile.

### 5.3.2. Effect of Length of the Pile on Lateral Load Capacity

To study the effect of length of the pile on lateral load capacity, 0.5, 0.8, 1.1, and 1.4m diameter piles of different lengths i.e. 15, 20, 25, and 30m were considered. The results indicate there is no any considerable change in lateral load capacity with increase in length except for pile diameter of 1.4m where there is a significant change from 15m pile length to 20m length because the pile is short pile and has small carrying capacity.

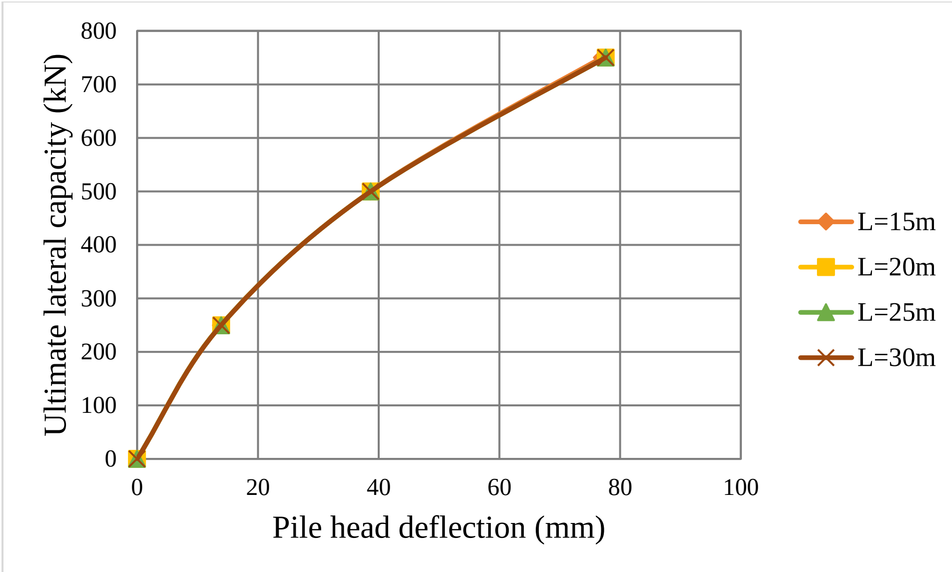


Figure 5.13: The effect of change in length on lateral capacity pile with diameter 0.5m.

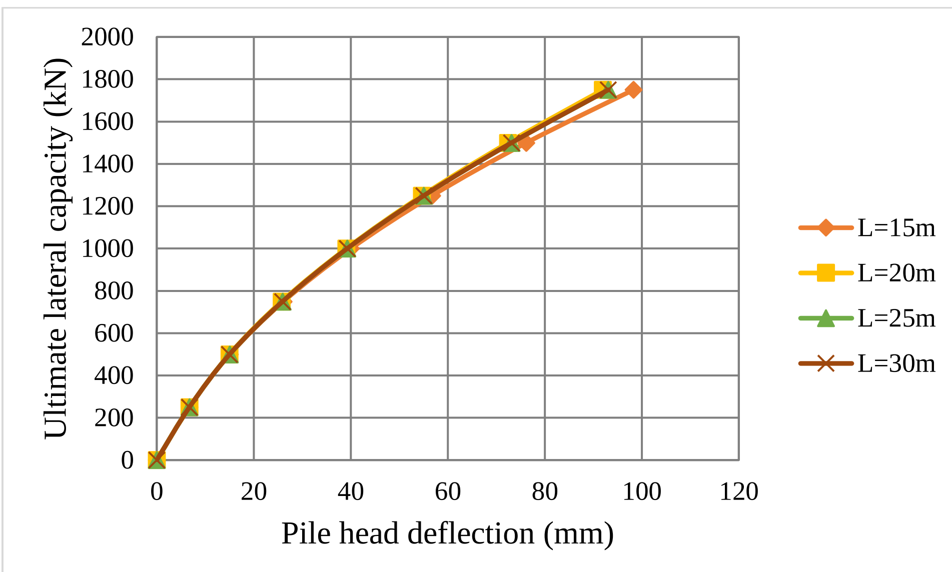


Figure 5.14: The effect of change in length on lateral capacity pile with diameter 0.8m.

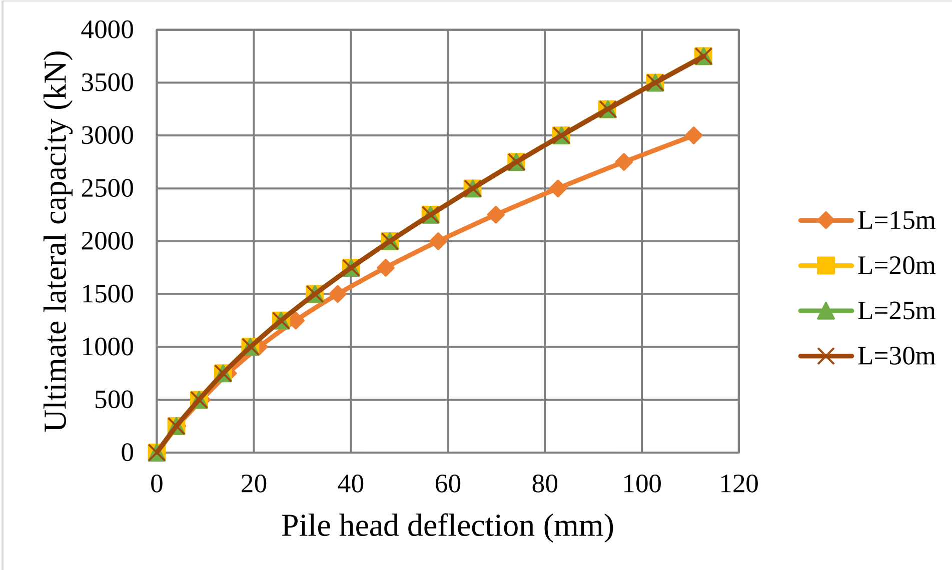


Figure 5.15: The effect of change in length on lateral capacity pile with diameter 1.1m.

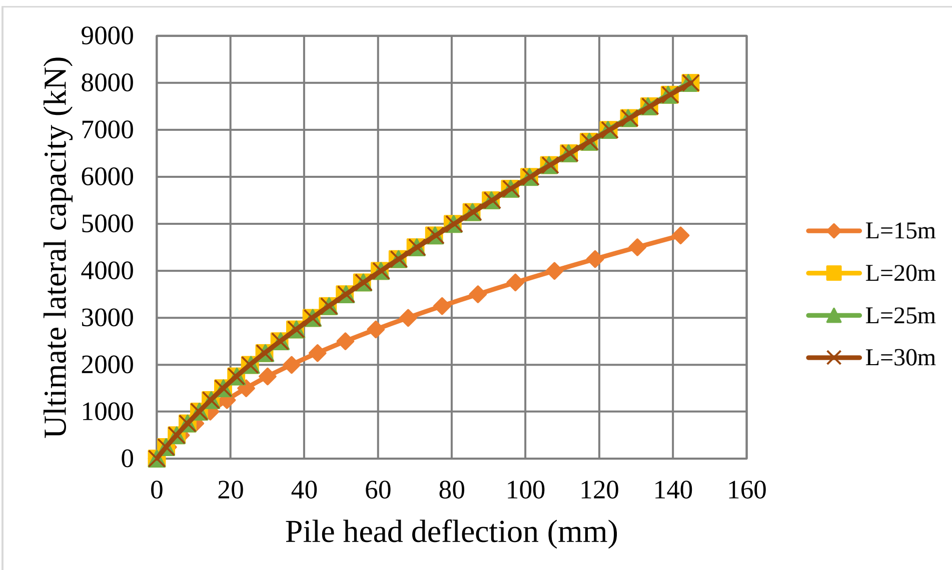


Figure 5.16: The effect of change in length on lateral capacity pile with diameter 1.4m.

Figures 5.13 to 5.16 show that ultimate lateral resistance is constant with increase in Length. This implies that with constant pile diameter and decreasing pile length, the ultimate lateral resistance of the pile remains unchanged. This is because the embedded length of the pile is greater than the critical length (Lc) of the pile.

# 6. CONCLUSIONS AND RECOMMENDATIONS

## 6.1. Conclusions

The main objective of this thesis was to study the lateral response of laterally loaded single pile embedded in layered soils considering the effect of pile diameter, pile length and loading eccentricity using PLAXIS 3D FOUNDATION.

A numerical model was developed using Plaxis 3D Foundation V1.1 software to analyze laterally loaded pile as three-dimensional problems. The model, accounts for the effect of pile diameter, pile length and loading eccentricity on the response of laterally loaded pile. The model was validated by comparing its results with the results of filed test available in the literature. The results of this numerical model were found in reasonable agreement with the results of field test available in the literature.

The results show that pile diameter and loading eccentricity significantly affect the response of laterally loaded piles. However, when the pile length is beyond the critical length, the finite element method results show that the response of laterally loaded pile is unchanged; the increase in pile length is insignificant. Loading eccentricity and the diameter of the pile greatly affects the response of the laterally loaded piles. The following conclusions have been made from the research.

- The head deflection of the pile decreased by 66.02%, 43.82% and 29.07% when the pile diameter increases from 500mm to 800mm, 800mm to 1100mm and 1100mm to 1400mm respectively with different pile length. Increase in diameter of pile reduces head deflection of the pile due to increase in structural stiffness.
- As anticipated, the lateral load capacity of pile increases by 62.14%, 48.36% and 36.51% when the pile diameter increases from 500mm to 800mm, 800mm to 1100mm and 1100mm to 1400mm respectively for different pile length since pile stiffness, EI, increases with increase in moment of inertia I, which depends on the diameter of pile.
- The head deflection, ultimate lateral capacity of laterally loaded pile remains constant with increase in length for constant pile diameter since the embedment length of pile is greater than its critical length.

- Increasing the load eccentricity from 0 to 1m, 1to 2m and 2 to 3m increases the pile head deflection by 34, 32 and 29% for the highest load respectively.
- From results of the study, the effect of pile length on the head deflection and ultimate lateral resistance was negligible. For economical design of laterally loaded pile, the selection of pile length is very important. For laterally loaded pile, the length of the pile is more than its critical length the design will be uneconomical.

## 6.2. Recommendations

The soil parameters required for numerical analysis used in this study were obtained from correlation of some geotechnical properties of soils and rocks, and taking typical values from different literatures. Only very limited parameters are directly taken from test result. This is due to lack of adequate laboratory and field test results for different soil layers at different depth. This can be raised as one significant drawback in this study. A better simulation result of FEM could have been obtained, if most soil parameters have been directly determined from laboratory and field test results.

In this thesis, static load was applied at the head of the pile. It is recommended to investigate the lateral performance of pile, when dynamic is applied on the pile and compare the effects with static load.

In this research, the dynamic behavior of the laterally loaded pile is not taken into consideration. Therefore, future study is required to consider the dynamic load and its effects on the lateral capacity and performance of laterally loaded pile.

# References

A.M.Trochanis, J.Bielak and P.Christiano. (1991). Three-dimensional nonlinear study of piles. *J. Geotech. Eng, 117*(3), 429–447.

B .McClelland and J. A. Jr.Focht. (1958a). *Soil modulus for laterally loaded piles.*

B.B.Broms. (1965). Design of laterally loaded piles. *J. Soil Mechanics and Foundations Division, ASCE*, *91*(SM3), 79-99.

B.Hansen, J. (1961). The ultimate resistance of rigid piles against transversal forces. *Bulletin, Danish Geotechnical Institue, Copenhagen, 11*, 5-9.

Basu, D., R. Salgado, and M. Prezzi. (2008). *Analysis of Laterally Loaded Piles in Multilayered Soil Deposits.* FHWA/IN/JTRP.

Briaud, J.-L. (2013). *Geotechnical Engineering: Unsaturated and Saturated Soil.* New Jersey Hoboken : John Wiley & Sons, Inc.

C.Desai and G.Appel. (1976). 3-D analysis of laterally loaded structures. *Proceedings of the 2nd International Conference on Numerical Methods in Geomechanics*, (pp. 405–418). Blacksburg.

C.Reese, L. (1986). *Behavior of Piles and Pile Groups Under Lateral Load.* Washington D.C: Federal Highway Administration.

D.A. Brown and C.F. Shie. (1990,1991). Three dimensional finite element model of laterally loaded piles. *Comput. Geotec*, *10*(1), 59–79.

D.A.Brown,M. Kumar,et al. (1989). PY curves for laterally loaded piles derived from three-dimensional finite element model. Numerical models in geomechanics. *Numog III. Proceedings of the 3rd International Symposium Held in Niagara falls*.

D.Douglas and E.Davis. (1964). The movement of buried footings due to moment and horizontal load and the movement of anchor plates. *Geotechnique*, *14*(2), 115–132.

E.A.Dickin and R.B.Nazir. (1999). Moment-carrying capacity of short pile foundations in cohesionless soil. *Geotechnical and Geoenvironmental Engineering ASCE*, *125*(1), 1-10.

E.Barber. (1953). Discussion to paper by SM Gleser. *154*, pp. 96–99 .

F.Ismael, N. (1998). Lateral loading tests on bored piles in cemented sands. *Proceedings of the 3rd International Geotchnical Seminar on Deep Foundation on Bored and Auger piles. 3rd*, pp. 137-144. Belguim: Ghent.

F.Scott, R. (1981). *Foundation Anaysis.* Prentice-Hall, Engel Wood Cliffs, NJ.

H.G.Poulos. (1971a,b). Behavior of laterally loaded piles. *Journal of Soil Mechanics and Foundation*, *97*(5), 711-751.

H.G.Poulos. (1973). Analysis of piles in soil undergoing lateral movement. *Journal of Soil Mechanics and Foundation Division*, *99*(5), 391–406.

H.G.Poulos and E.H.Davis. (1980). *Pile Foundation Analysis and Design.* New York: Wiley and Sons.

H.G.Poulos and T.S.Hull. (1989). The role of analytical mechanics in foundation. *Foundation Engineering, Current Principals and Practices.*

H.Matlock and L.C.Reese. (1960). Generalized solutions for laterally loaded piles. *Journal of Soil Mechanics and Foundations Division, 86*(5), 63–94.

J.R.Peng, M.Rouainia,and B.Clarke. (2010). Finite element analysis of laterally loaded fin piles. *Comput. Struct, 88*(21), 1239–1247.

K.Yang and R.Liang. (2006). A 3D FEM model for laterally loaded drilled shafts in rock. *Int. GeoCongress 2006@ sGeotechnical Engineering in the Information Technology Age*, 1–6.

Ken Fleming Ken, Austin Weltman,Mark Randolph and Keith Elson. (2009). *Piling Engineering* (3rd ed.). London and New York: Taylor & Francis.

Lemesa, Z. (2019). *Analysis and Parametric Study of Tangent Pile Wall as Deep Excavation Support System Using Finite Element Based Software.*

Lymon C. Reese and Hudson Matlock. (1956). Nondimensional solutions for laterally loaded piles with soil modulus assumed proportional to depth. *Proceedings of the VIII Texas Conference on Soil Mechanics and Foundation Engineering.* Austin: University of Texas.

Lymon C.Reese and William F.Van Impe. (2011). *Single Piles and Pile Groups under Lateral Loading.* CRC Press Taylor & Francis Group Boca Rotan.

M.A.Biot. (1937). Bending of an infinite beam on an elastic foundation. *Journal of Applied Mechanics, 2(3)*, 165–184.

M.Ahmadi and S.Ahmari. (2009). Finite-element modelling of laterally loaded piles in clay. *162*(3), 151–163.

M.Budhu and T.G.Davies. (1987,1988). Nonlinear analysis of laterality loaded piles in cohesionless soils. *Canadian Geotechnical Journal*, *24*(2), 289–296.

M.F.Randolph. (1981). The response of flexible piles to lateral loading. *Geotechnique, 31*(2), 247–259.

M.Faruque and C.Desai. (1982). 3-D material and geometric nonlinear analysis of piles. *Proceedings of the Second International Conference on Numerical Methods in Offshore Pilling*, 553–575.

M.Hetenyi. (1946). *Beams on Elastic Foundation.* The University of Michigan Press.

M.Jamiolkowski and A.Garassino. (1977). Soil modulus for laterally loaded piles. *In Proceedings of the Specialty Session 10, Ninth International Conference on Soil Mechanics and Foundation Engineering*, (pp. 43-58). Tokyo.

M.Mardfekri, P.Gardoni and J.M. Rosset. (2013). Modeling laterally loaded single piles accounting for nonlinear soil-pile interactions. *J. Eng, 3*, 1-7.

M.Wood, D. (1990). *Soil Behaviour and Critical State Soil Mechanics.* New York: Cambridge University Press.

P.K.Banerjee and T.G Davis. (1978). The behaviour of axially and laterally loaded single piles embedded in non-homogeneous soils. *Geotechnique, 28*, 309–326.

P.Kavitha, K.Beena and K.Narayanan. (2016). A review on soil–structure interaction analysis of laterally loaded piles. *Innov. Infrastruct. Solut, 1*, 1-15.

P.W.Rowe. (1956). The single pile subject to horizontal force. *Géotechnique, 6*(2), 70-85.

R.B.J. Brinkgreve and W. Broere. (2006). *Plaxis 3D Foundation Reference Manual Version 1.5.* DELFT, Netherlands.

R.D.Mindlin. (1936). Force at a point in the interior of a semi-infinite solid. *Journal of Applied Physics, 7*(5), 195–202.

R.Tuladhar, H. Mutsuyoshi and T.Maki. (2013). Numerical modelling and full-scale testing of concrete piles under lateral loading. *Aust. J. Struct. Eng, 14*(3), 229–242 .

Rollins K.M. and Sparks A.E. (2002). Lateral Resistance of full scale pile cap with gravel backfill. *Geotechnical and Geoenvironmental Engineering, 128*(9), 711-723.

S. Karthigeyan, V. V. G. S. T. Ramakrishna and K. Rajagopal. (2007). Numerical investigation of the effect of vertical load on the. *Journal of Geotechnical and Geoenvironmental Engineering, Vol. 133, No. 5,* .

Sawwaf, M. E. (2006). Lateral Resistance of Single Pile Located Near Geosynthetic Reinforced Slope. *Geotechnical and Geoenvironmental Engineering*.

T.Davies and M.Budhu. (1986). Non-linear analysis of laterally loaded piles in heavily overconsolidated clays. *Geotechnique, 36*(4), 527–538.

Terzaghi, K. (1955). Evaluation of coefficient of subgrade reaction. *Geotechniques, 5(4)*, 297-326.

W.R.Spillers and R.D.Stoll. (1964). Lateral response of piles. *Journal of Soil Mechanics and Foundation Division, 90*(6), 1–10.

Z.Yang and B.Jeremi. (2005). Study of soil layering effects on lateral loading behavior of piles. . *Geotech. Geoenviron. Eng, 131*(6), 762–770 .

# Appendix A - Geotechnical properties of soil

**Typical values of soil Young's modulus for different soils according to USCS.**

In general, the soil stiffness and elastic modulus depends on the consistency and the parking (density) of the soil. Typical values of soil Young's modulus are given below as guideline.

Table A. 1: Typical values SPT - Based soil and rock classification systems (Skempton, 1986)

| | | |
|---|---|---|
| Sand | $N_{60}$<br>0-3<br>3-8<br>8-25<br>25-42<br>42-58 | <br>Very Loose<br>Loose<br>Medium<br>Dense<br>Very Dense |
| Clays | $N_{60}$<br>0-4<br>4-8<br>8-15<br>15-30<br>30-60<br>>60 | <br>Very Soft<br>soft<br>Firm<br>Stiff<br>Very Stiff<br>Hard |
| Week Rock | $N_{60}$<br>0-80<br>80-200<br>>200 | <br>Very Weak<br>Weak<br>Moderately<br>Weak to Very Strong |

Table A .2: Typical values of Young's modulus (MPa) for granular materials (Kézdi&Réthāti, 1974 and Prat et al., 1995)

| USCS | Description | Loose | Medium | Dense |
|---|---|---|---|---|
| GW, SW | Gravels/Sand well-graded | 30-80 | 80-160 | 160-320 |
| SP | Sand, uniform | 10-30 | 30-50 | 50-80 |
| GM, SM | Sand/Gravel silty | 7-12 | 12-20 | 20-30 |

Table A.3: Typical values of Young's modulus (MPa) for cohesive materials (Kézdi and Rétháti, 1974 and Prat et al., 1995)

| USCS | Description | Very soft to soft | Medium | Stiff to very stiff | Hard |
|---|---|---|---|---|---|
| ML | Silts with slight plasticity | 2.5 – 8 | 10 – 15 | 15 -40 | 40 – 80 |
| ML, CL | Silts with low plasticity | 1.5 – 6 | 6 -10 | 10 – 30 | 30 -60 |
| CL | Clays with low-medium plasticity | 0.5 – 5 | 5 -8 | 8 – 30 | 30 – 70 |
| CH | Clays with high plasticity | 0.35 – 4 | 4 -7 | 7 – 20 | 20 – 32 |
| OL | Organic silts | - | 0.5 -5 | - | - |
| OH | Organic clays | - | 0.5 -4 | - | - |

Table A.4: Typical values of Poisson's ratio for soils and other material, Bowels (1977)

| **Types of Soils** | $\nu$ |
|---|---|
| Clay (Saturated) | 0.4-0.5 |
| Clay (Unsaturated) | 0.1-0.3 |
| Sandy Clay | 0.2-0.3 |
| Silt | 0.3-0.35 |
| Sand- Dense | 0.2-0.4 |
| Sand -Coarse (Void Ratio=0.4-0.7) | 0.15 |
| Sand-Fine (Void Ratio=0.4-0.7) | 0.25 |
| Rock | 0.1-0.4 (Depending on type of Rock) |
| Loess | 0.1-0.3 |
| Ice | 0.36 |
| Concrete | 0.15 |

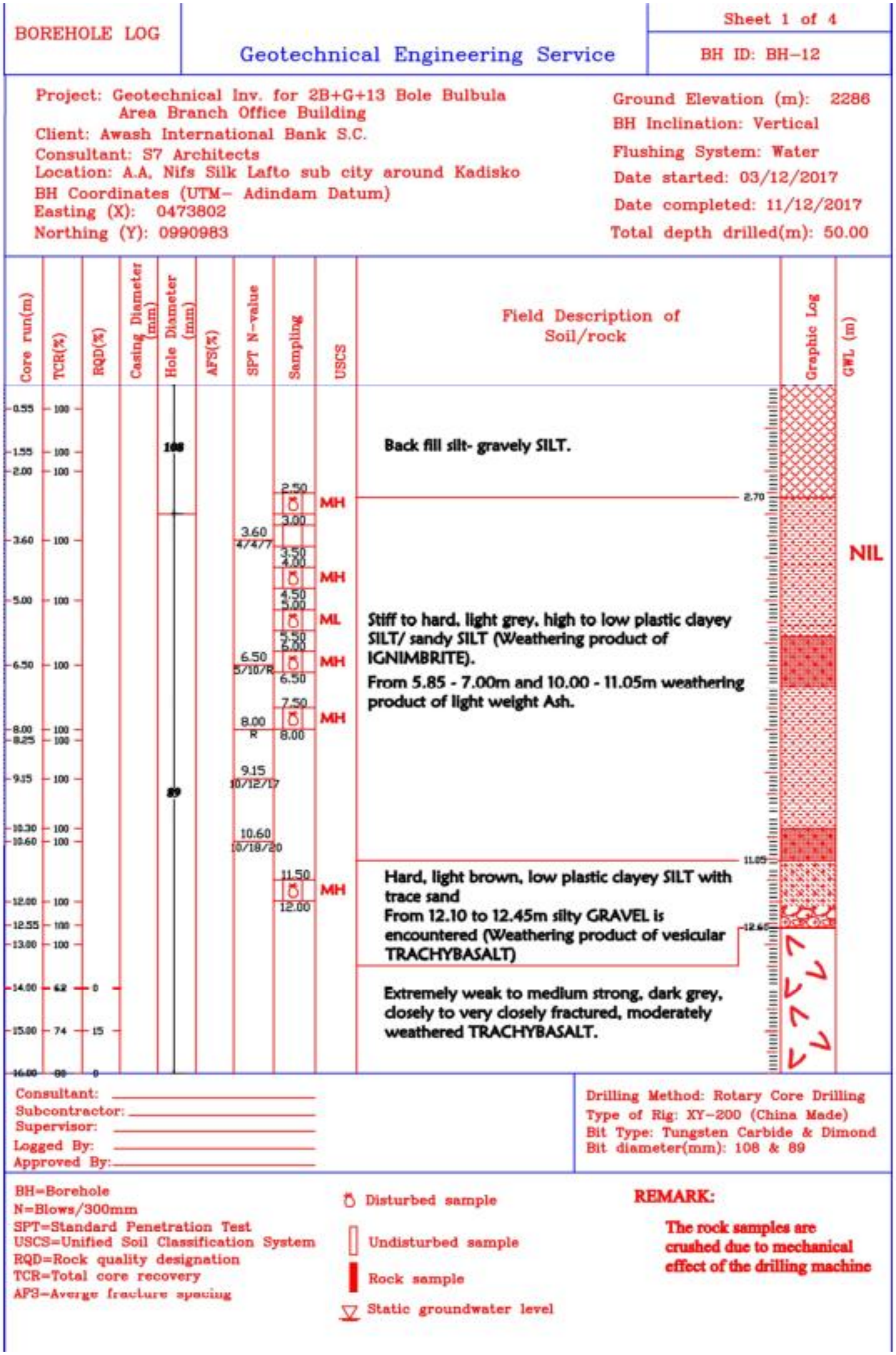
BOREHOLE LOG
Geotechnical Engineering Service
Sheet 1 of 4
BH ID: BH–12
Project: Geotechnical Inv. for 2B+G+13 Bole Bulbula Area Branch Office Building
Client: Awash International Bank S.C.
Consultant: S7 Architects
Location: A.A, Nifs Silk Lafto sub city around Kadisko
BH Coordinates (UTM– Adindam Datum)
Easting (X): 0473802
Northing (Y): 0990983
Ground Elevation (m): 2286
BH Inclination: Vertical
Flushing System: Water
Date started: 03/12/2017
Date completed: 11/12/2017
Total depth drilled(m): 50.00
Core run(m)
TCR(%)
RQD(%)
Casing Diameter (mm)
Hole Diameter (mm)
AFS(%)
SPT N-value
Sampling
USCS
Field Description of Soil/rock
Graphic Log
GWL (m)
0.55
1.55
2.00
3.60
5.00
6.50
8.00
8.25
9.35
10.30
10.60
12.00
12.55
13.00
14.00
15.00
16.00
100
62
74
0
15
108
89
2.50
3.00
3.50
4.00
4.50
5.00
5.50
6.00
6.50
7.50
8.00
11.50
12.00
3.60 4/4/7
6.50 5/10/R
8.00 R
9.15 10/12/17
10.60 10/18/20
MH
ML
Back fill silt- gravely SILT.
2.70
Stiff to hard, light grey, high to low plastic clayey SILT/ sandy SILT (Weathering product of IGNIMBRITE).
From 5.85 - 7.00m and 10.00 - 11.05m weathering product of light weight Ash.
11.05
Hard, light brown, low plastic clayey SILT with trace sand
From 12.10 to 12.45m silty GRAVEL is encountered (Weathering product of vesicular TRACHYBASALT)
12.45
Extremely weak to medium strong, dark grey, closely to very closely fractured, moderately weathered TRACHYBASALT.
NIL
Consultant:
Subcontractor:
Supervisor:
Logged By:
Approved By:
Drilling Method: Rotary Core Drilling
Type of Rig: XY–200 (China Made)
Bit Type: Tungsten Carbide & Dimond
Bit diameter(mm): 108 & 89
BH=Borehole
N=Blows/300mm
SPT=Standard Penetration Test
USCS=Unified Soil Classification System
RQD=Rock quality designation
TCR=Total core recovery
AFS=Averge fracture spacing
Disturbed sample
Undisturbed sample
Rock sample
Static groundwater level
REMARK:
The rock samples are crushed due to mechanical effect of the drilling machine

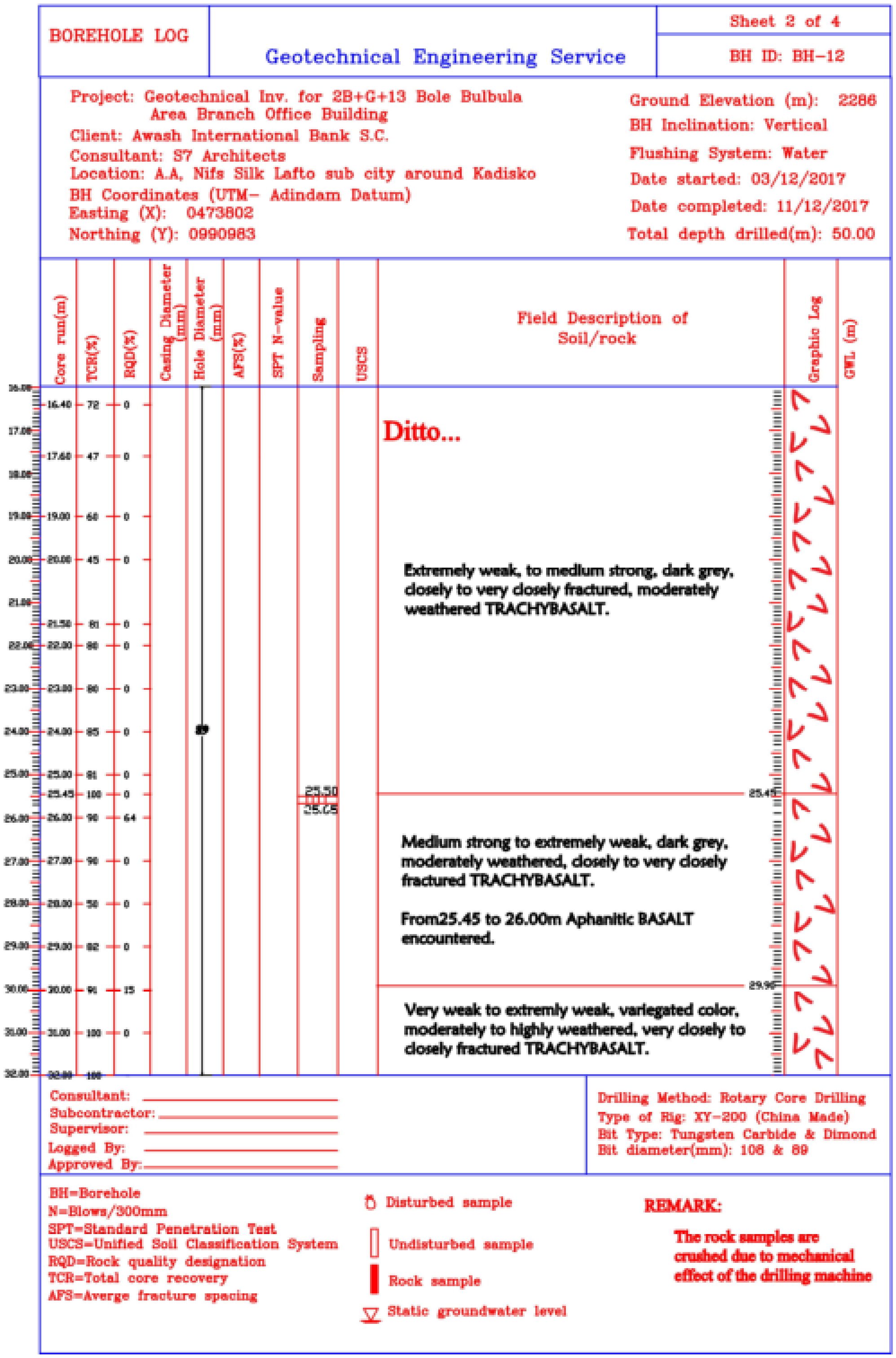
BOREHOLE LOG
Geotechnical Engineering Service
Sheet 2 of 4
BH ID: BH-12
Project: Geotechnical Inv. for 2B+G+13 Bole Bulbula Area Branch Office Building
Client: Awash International Bank S.C.
Consultant: S7 Architects
Location: A.A, Nifs Silk Lafto sub city around Kadisko
BH Coordinates (UTM- Adindam Datum)
Easting (X): 0473802
Northing (Y): 0990983
Ground Elevation (m): 2286
BH Inclination: Vertical
Flushing System: Water
Date started: 03/12/2017
Date completed: 11/12/2017
Total depth drilled(m): 50.00
Core run(m)
TCR(%)
RQD(%)
Casing Diameter (mm)
Hole Diameter (mm)
AFS(%)
SPT N-value
Sampling
USCS
Field Description of Soil/rock
Graphic Log
GWL (m)
Ditto...
Extremely weak, to medium strong, dark grey, closely to very closely fractured, moderately weathered TRACHYBASALT.
Medium strong to extremely weak, dark grey, moderately weathered, closely to very closely fractured TRACHYBASALT.
From25.45 to 26.00m Aphanitic BASALT encountered.
Very weak to extremly weak, variegated color, moderately to highly weathered, very closely to closely fractured TRACHYBASALT.
25.45
29.90
25.50
25.05
Consultant:
Subcontractor:
Supervisor:
Logged By:
Approved By:
Drilling Method: Rotary Core Drilling
Type of Rig: XY-200 (China Made)
Bit Type: Tungsten Carbide & Dimond
Bit diameter(mm): 108 & 89
BH=Borehole
N=Blows/300mm
SPT=Standard Penetration Test
USCS=Unified Soil Classification System
RQD=Rock quality designation
TCR=Total core recovery
AFS=Averge fracture spacing
Disturbed sample
Undisturbed sample
Rock sample
Static groundwater level
REMARK:
The rock samples are crushed due to mechanical effect of the drilling machine

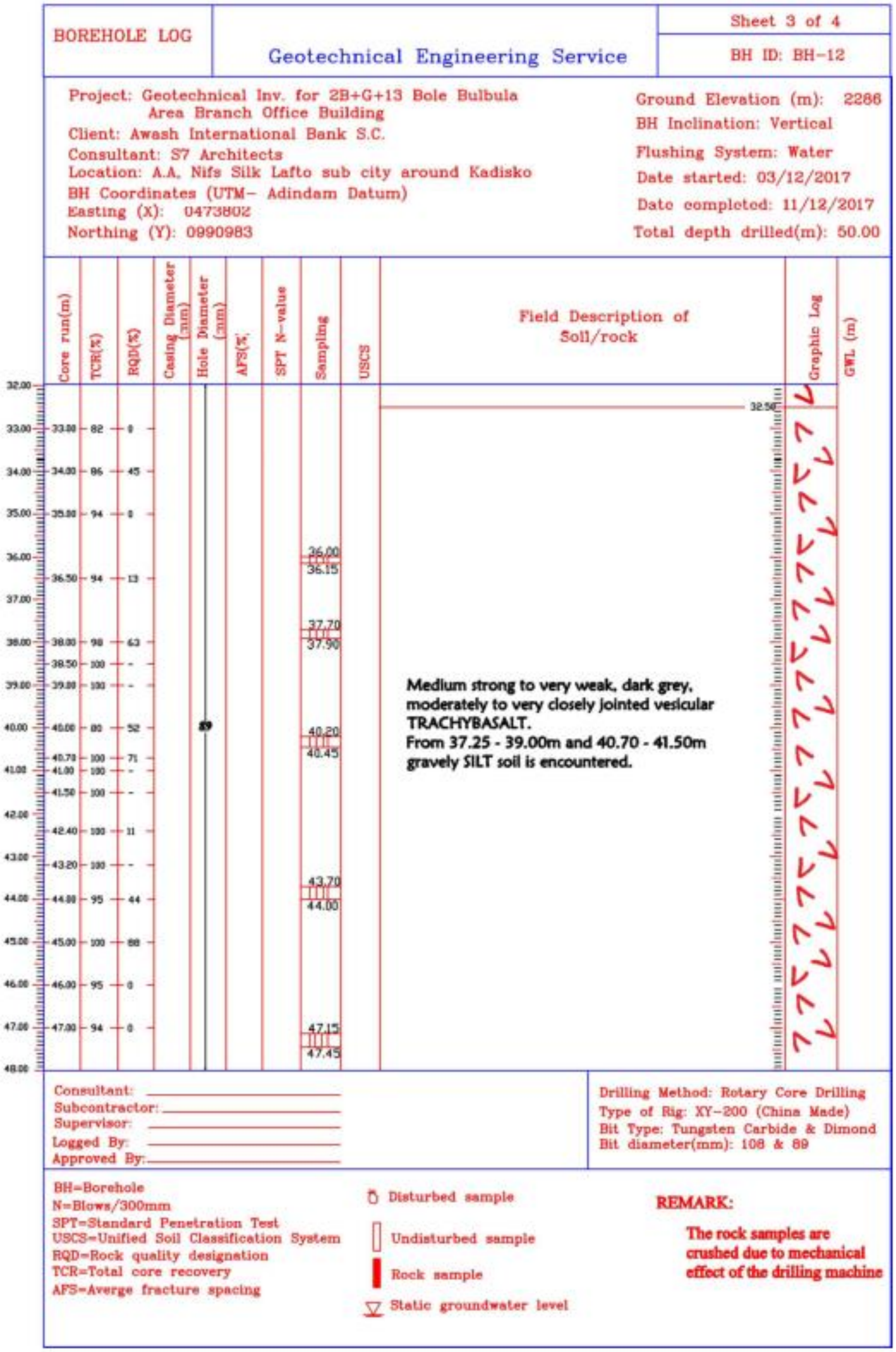


Figure A.1:Borehole log sheet

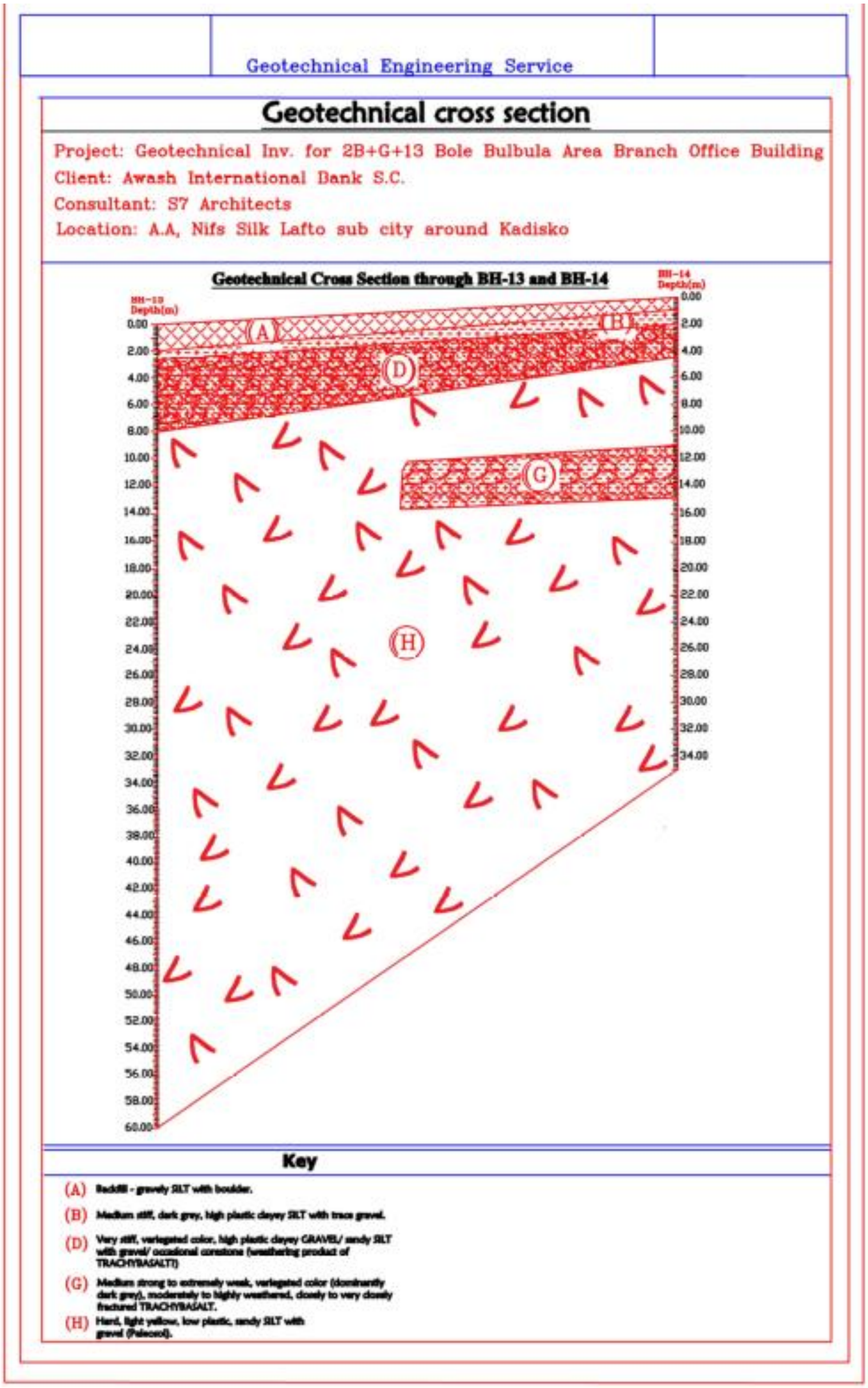


Figure A.2: Cross section

# Appendix B - Ultimate Capacity from Numerical Results

Table B.1: Lateral load capacity and lateral deflection

| Length of Pile (m) | Pile Diameter(m) | L/D Ratio | Lateral load capacity (KN) | Lateral deflection (mm) |
|---|---|---|---|---|
| 15 | 0.5 | 30.00 | 584.03 | 50 |
| 15 | 0.8 | 18.75 | 1542.82 | 80 |
| 15 | 1.1 | 13.64 | 2987.65 | 110 |
| 15 | 1.4 | 10.71 | 4706.00 | 140 |
| 20 | 0.5 | 40.00 | 572.58 | 50 |
| 20 | 0.8 | 25.00 | 1596.85 | 80 |
| 20 | 1.1 | 18.18182 | 3682.93 | 110 |
| 20 | 1.4 | 14.28571 | 7788.01 | 140 |
| 25 | 0.5 | 50 | 572.58 | 50 |
| 25 | 0.8 | 31.25 | 1585.72 | 80 |
| 25 | 1.1 | 22.72727 | 3680.68 | 110 |
| 25 | 1.4 | 17.85714 | 7809.31 | 140 |
| 30 | 0.5 | 60 | 572.58 | 50 |
| 30 | 0.8 | 37.5 | 1585.80 | 80 |
| 30 | 1.1 | 27.27273 | 3680.36 | 110 |
| 30 | 1.4 | 21.42857 | 7780.63 | 140 |

# Appendix C- Plaxis out

Table C.1: Pile length of 15m

| Pile Length=15m | | | | | | | |
|---|---|---|---|---|---|---|---|
| Pile diameter = 0.5m | | Pile diameter = 0.8m | | Pile diameter = 1.1m | | Pile diameter = 1.4m | |
| Lateral load (KN) | Pile head deflection(mm) | Lateral load (KN) | Pile head deflection(mm) | Lateral load (KN) | Pile head deflection(mm) | Lateral load (KN) | Pile head deflection(mm) |
| 0 | 0 | 0 | 0 | 0 | 0 | 0 | 0 |
| 250 | 13.88 | 250 | 6.75 | 250 | 4.26 | 250 | 3.06 |
| 500 | 38.63 | 500 | 15.07 | 500 | 9.23 | 500 | 6.56 |
| 750 | 76.96 | 750 | 26.15 | 750 | 14.69 | 750 | 10.42 |
| | | 1000 | 40.04 | 1000 | 21.1 | 1000 | 14.53 |
| | | 1250 | 56.77 | 1250 | 28.67 | 1250 | 19.03 |
| | | 1500 | 76.22 | 1500 | 37.33 | 1500 | 24.26 |
| | | 1750 | 98.29 | 1750 | 47.18 | 1750 | 30.04 |
| | | | | 2000 | 58.04 | 2000 | 36.56 |
| | | | | 2250 | 69.89 | 2250 | 43.59 |
| | | | | 2500 | 82.72 | 2500 | 51.19 |
| | | | | 2750 | 96.34 | 2750 | 59.41 |
| | | | | 3000 | 110.71 | 3000 | 68.16 |
| | | | | | | 3250 | 77.42 |
| | | | | | | 3500 | 87.15 |
| | | | | | | 3750 | 97.29 |
| | | | | | | 4000 | 107.89 |
| | | | | | | 4250 | 118.9 |
| | | | | | | 4500 | 130.32 |
| | | | | | | 4750 | 142.04 |

Table C.2: Pile length of 20m

| Pile Length=20m | | | | | | | |
|---|---|---|---|---|---|---|---|
| Pile diameter = 0.5m | | Pile diameter = 0.8m | | Pile diameter = 1.1m | | Pile diameter = 1.4m | |
| Lateral load (KN) | Pile head deflection(mm) | Lateral load (KN) | Pile head deflection(mm) | Lateral load (kN) | Pile head deflection(mm) | Lateral load (KN) | Pile head deflection(mm) |
| 0 | 0 | 0 | 0 | 0 | 0 | 0 | 0 |
| 250 | 13.9 | 250 | 6.74 | 250 | 4.06 | 250 | 2.56 |
| 500 | 38.71 | 500 | 14.98 | 500 | 8.7 | 500 | 5.37 |
| 750 | 77.6 | 750 | 25.76 | 750 | 13.69 | 750 | 8.35 |
| | | 1000 | 39.1 | 1000 | 19.32 | 1000 | 11.45 |
| | | 1250 | 54.7 | 1250 | 25.62 | 1250 | 14.64 |
| | | 1500 | 72.43 | 1500 | 32.59 | 1500 | 17.98 |
| | | 1750 | 91.97 | 1750 | 40.07 | 1750 | 21.55 |
| | | | | 2000 | 48.04 | 2000 | 25.29 |
| | | | | 2250 | 56.42 | 2250 | 29.2 |
| | | | | 2500 | 65.11 | 2500 | 33.3 |
| | | | | 2750 | 74.11 | 2750 | 37.55 |
| | | | | 3000 | 83.38 | 3000 | 41.92 |
| | | | | 3250 | 92.92 | 3250 | 46.41 |
| | | | | 3500 | 102.69 | 3500 | 50.98 |
| | | | | 3750 | 112.68 | 3750 | 55.64 |
| | | | | | | 4000 | 60.44 |
| | | | | | | 4250 | 65.31 |
| | | | | | | 4500 | 70.22 |
| | | | | | | 4750 | 75.19 |
| | | | | | | 5000 | 80.27 |
| | | | | | | 5250 | 85.39 |
| | | | | | | 5500 | 90.56 |
| | | | | | | 5750 | 95.78 |
| | | | | | | 6000 | 101.03 |
| | | | | | | 6250 | 106.37 |
| | | | | | | 6500 | 111.74 |
| | | | | | | 6750 | 117.15 |
| | | | | | | 7000 | 122.58 |
| | | | | | | 7250 | 128.06 |
| | | | | | | 7500 | 133.59 |

| | | | | | | | |
|---|---|---|---|---|---|---|---|
| | | | | | | 7750 | 139.15 |
| | | | | | | 8000 | 144.74 |

Table C.3: Pile length of 25m

| Pile Length=25m | | | | | | | |
|---|---|---|---|---|---|---|---|
| Pile diameter = 0.5m | | Pile diameter = 0.8m | | Pile diameter = 1.1m | | Pile diameter = 1.4m | |
| Lateral load (KN) | Pile head deflection(mm) | Lateral load (KN) | Pile head deflection(mm) | Lateral load (KN) | Pile head deflection(mm) | Lateral load (KN) | Pile head deflection(mm) |
| 0 | 0 | 0 | 0 | 0 | 0 | 0 | 0 |
| 250 | 13.9 | 250 | 6.74 | 250 | 4.05 | 250 | 2.57 |
| 500 | 38.71 | 500 | 15.04 | 500 | 8.71 | 500 | 5.39 |
| 750 | 77.6 | 750 | 25.97 | 750 | 13.69 | 750 | 8.4 |
| | | 1000 | 39.28 | 1000 | 19.32 | 1000 | 11.53 |
| | | 1250 | 55.06 | 1250 | 25.63 | 1250 | 14.77 |
| | | 1500 | 73.17 | 1500 | 32.6 | 1500 | 18.12 |
| | | 1750 | 93.09 | 1750 | 40.09 | 1750 | 21.71 |
| | | | | 2000 | 48.07 | 2000 | 25.53 |
| | | | | 2250 | 56.47 | 2250 | 29.5 |
| | | | | 2500 | 65.17 | 2500 | 33.64 |
| | | | | 2750 | 74.17 | 2750 | 37.92 |
| | | | | 3000 | 83.46 | 3000 | 42.29 |
| | | | | 3250 | 92.99 | 3250 | 46.76 |
| | | | | 3500 | 102.78 | 3500 | 51.34 |
| | | | | 3750 | 112.77 | 3750 | 56.02 |
| | | | | | | 4000 | 60.77 |
| | | | | | | 4250 | 65.61 |
| | | | | | | 4500 | 70.52 |
| | | | | | | 4750 | 75.49 |
| | | | | | | 5000 | 80.53 |
| | | | | | | 5250 | 85.63 |
| | | | | | | 5500 | 90.75 |
| | | | | | | 5750 | 95.93 |
| | | | | | | 6000 | 101.13 |
| | | | | | | 6250 | 106.39 |
| | | | | | | 6500 | 111.7 |
| | | | | | | 6750 | 117.29 |
| | | | | | | 7000 | 122.39 |
| | | | | | | 7250 | 127.81 |

| | | | | | | | |
|---|---|---|---|---|---|---|---|
| | | | | | | 7500 | 133.24 |
| | | | | | | 7750 | 138.7 |
| | | | | | | 8000 | 144.18 |

Table C.4: Pile length of 30m

| Pile Length=30m | | | | | | | |
|---|---|---|---|---|---|---|---|
| Pile diameter = 0.5m | | Pile diameter = 0.8m | | Pile diameter = 1.1m | | Pile diameter = 1.4m | |
| Lateral load (KN) | Pile head deflection (mm) | Lateral load (KN) | Pile head deflection(mm) | Lateral load (KN) | Pile head deflection(mm) | Lateral load (KN) | Pile head deflection(mm) |
| 0 | 0 | 0 | 0 | 0 | 0 | 0 | 0 |
| 250 | 13.92 | 250 | 6.74 | 250 | 4.06 | 250 | 2.56 |
| 580 | 49.42 | 500 | 15.03 | 500 | 8.71 | 500 | 5.37 |
| 588 | 50.57 | 750 | 25.96 | 750 | 13.69 | 750 | 8.36 |
| | | 1000 | 39.28 | 1000 | 19.34 | 1000 | 11.47 |
| | | 1250 | 55.05 | 1250 | 25.64 | 1250 | 14.67 |
| | | 1500 | 73.16 | 1500 | 32.61 | 1500 | 18.02 |
| | | 1750 | 93.09 | 1750 | 40.09 | 1750 | 21.57 |
| | | | | 2000 | 48.07 | 2000 | 25.3 |
| | | | | 2250 | 56.46 | 2250 | 29.29 |
| | | | | 2500 | 65.17 | 2500 | 33.49 |
| | | | | 2750 | 74.18 | 2750 | 37.8 |
| | | | | 3000 | 83.47 | 3000 | 42.2 |
| | | | | 3250 | 93.02 | 3250 | 46.72 |
| | | | | 3500 | 102.8 | 3500 | 51.35 |
| | | | | 3750 | 112.78 | 3750 | 56.08 |
| | | | | | | 4000 | 60.87 |
| | | | | | | 4250 | 65.7 |
| | | | | | | 4500 | 70.63 |
| | | | | | | 4750 | 75.65 |
| | | | | | | 5000 | 80.72 |
| | | | | | | 5250 | 85.83 |
| | | | | | | 5500 | 91 |
| | | | | | | 5750 | 96.16 |
| | | | | | | 6000 | 101.44 |
| | | | | | | 6250 | 106.71 |
| | | | | | | 6500 | 112.05 |
| | | | | | | 6750 | 117.43 |
| | | | | | | 7000 | 122.85 |

| | | | | | | | |
|---|---|---|---|---|---|---|---|
| | | | | | | 7250 | 128.31 |
| | | | | | | 7500 | 133.8 |
| | | | | | | 7750 | 139.32 |
| | | | | | | 8000 | 144.87 |